NASA
Technical
Memorandum

NASA TM-86469

STUDIES OF SOLAR MAGNETIC FIELDS DURING THE SOLAR MAXIMUM YEAR

By M. J. Hagyard
Space Science Laboratory

September 1984

National Aeronautics and
Space Administration

George C. Marshall Space Flight Center

MSFC - Form 3190 (Rev. May 1983)

TECHNICAL REPORT STANDARD TITLE PAGE

1. REPORT NO.	2. GOVERNMENT ACCESSION NO.	3. RECIPIENT'S CATALOG NO.
NASA TM-86469		

4. TITLE AND SUBTITLE	5. REPORT DATE
Studies of Solar Magnetic Fields During the Solar Maximum Year	September 1984
	6. PERFORMING ORGANIZATION CODE
7. AUTHOR(S)	8. PERFORMING ORGANIZATION REPORT #
M. J. Hagyard	
9. PERFORMING ORGANIZATION NAME AND ADDRESS	10. WORK UNIT NO.
George C. Marshall Space Flight Center Marshall Space Flight Center, Alabama 35812	11. CONTRACT OR GRANT NO.
	13. TYPE OF REPORT & PERIOD COVERED
12. SPONSORING AGENCY NAME AND ADDRESS	Technical Memorandum
National Aeronautics and Space Administration Washington, D.C. 20546	14. SPONSORING AGENCY CODE

15. SUPPLEMENTARY NOTES

Prepared by Space Science Laboratory, Science and Engineering Directorate.

16. ABSTRACT

This report is a review of observations and studies of solar magnetic fields that were carried out during the period of the Solar Maximum Year (SMY), January 1980 to June 1981, with the goal of providing an overview of what was learned about solar magnetic fields during the SMY. The review covers the subjects of the relationship between solar magnetic fields and flares, the role of magnetic fields in the sunspot phenomenon, the magnetic-canopy structure overlying the supergranular network as well as the turbulent magnetic fields within the network, the fields within the polar crown prominences, and the solar magnetic cycle.

17. KEY WORDS	18. DISTRIBUTION STATEMENT
Solar Magnetic Fields Solar Maximum Year	Unclassified — Unlimited

19. SECURITY CLASSIF. (of this report)	20. SECURITY CLASSIF. (of this page)	21. NO. OF PAGES	22. PRICE
Unclassified	Unclassified	60	NTIS

MSFC - Form 3292 (May 1969)

For sale by National Technical Information Service, Springfield, Virginia 22151

ACKNOWLEDGMENTS

The author is extremely grateful for the many contributions which were submitted for this review. All of the material which was received was studied with extreme interest; the omission of some material from this paper reflects the limited scope of the review topic and not a lack of interest.

TABLE OF CONTENTS

LIST OF ILLUSTRATIONS

LIST OF ILLUSTRATIONS (Continued)

LIST OF ILLUSTRATIONS (Concluded)

TECHNICAL MEMORANDUM

STUDIES OF SOLAR MAGNETIC FIELDS DURING THE SOLAR MAXIMUM YEAR

I. INTRODUCTION

During the General Assembly of the International Astronomical Union (IAU) in Patras, Greece, in August 1982, Commission 10 of the IAU organized a special session on the scientific results of the Solar Maximum Year (SMY) which covered the interval January 1980 to June 1981. Invited presentations were given relating to different aspects of the SMY and covering both ground-based and spaceborne observations. Among the topics presented were reports of Flare Buildup Study (FBS), Study of Energy Release in Flares (SERF), and Study of Traveling Interplanetary Phenomena (STIP) activities world-wide; reviews of the Hinotori and Solar Maximum Mission (SMM) satellite observations; and reviews of radio astronomical and magnetic field studies during the SMY. The latter review is the subject of this report which represents an extended version of the paper presented at the Patras meeting.

The scope of this report does not encompass all the research in solar magnetic fields carried out during the SMY; rather the report in essence is a compilation of the observations and studies of solar magnetic fields which were reported to the author by the many contributors world-wide who are involved in this area of research. Among the material contributed, emphasis has been given to new results that are pertinent to the objectives of the SMY, with the goal of providing an overview of what has been learned about magnetic fields during the SMY.

II. MAGNETIC FIELDS AND SOLAR FLARES

For well over a decade, the free energy stored in stressed magnetic fields has been considered the primary source of the energy released in solar flares. Storage of this energy is perceived as a result of the evolution of magnetic field loops from potential to force-free configurations in the upper atmosphere. This evolution can occur through the shearing of magnetic loops as a result of footpoint translations or twisting of individual loops rooted in sunspots which undergo rotational motion. Release of the stored energy results from the development of an instability which causes a reduction or destruction of the currents associated with these stressed loops. Mechanisms for the onset of instability include evolution of stressed loops into non-equilibrium configurations or emergence of new flux near stressed loops. It seems clear then that observations of the solar magnetic field should give us insight as to what mechanisms are operative.

A. Energy Buildup Through Stressed Fields

It is well known that rapidly developing active regions with the attendant spot motions usually observed are prime candidates for producing flares. This correlation provides indirect evidence for the buildup of flare energy by the stressing of interconnecting fields between the moving spots. Figure 1 is an excellent example, from

the Yunnan Observatory (Hong et al., [1]) in China, of the rapid development of three sunspots through the coalescence of several smaller spots. This active region, Boulder number 2372, was born on the solar disk early on April 4, 1980, and produced many flares during its period of growth and development. From the Yunnan observations, sunspot pictures were obtained at 1 to 3 hr intervals on April 5 from 0050 to 0915 UT (Fig. 1a). Using these pictures, the relative sunspot motions that occurred between observations were deduced and are shown in Figure 1b. These moving sunspots were shown to be spatially grouped into three sectors, with the spots in each sector moving in converging directions to coalesce into one of the three primary sunspots seen on April 6. Since these motions involved spots of different magnetic polarities, it is certain that the interconnecting fields were stretched or sheared, with energy buildup occurring in the process.

More indirect evidence for preflare energy storage in stressed fields comes from observed changes in H-alpha fibrils during the course of a solar flare; the fibrils presumably delineate the chromospheric magnetic field. In a detailed study of the August 1972 flares, Zirin and Tanaka [2] infer the presence of strongly-sheared, transverse magnetic fields from the twisted appearance of penumbral filaments. Based on these observations, Tanaka and Nakagawa [3] obtained quantitative estimates of the available force-free magnetic energy as a function of the degree of shear. The temporal and spatial changes in fibril geometry were documented in detail by Neidig [4] over the interval of a subflare of September 14, 1977. In that study, Neidig illustrated the localized nature of the fibril changes and showed that these field relaxations occur even in the smallest flares.

Direct evidence of twisted or sheared magnetic loops can be derived from measurements of the vector magnetic field in the photosphere. Specifically, directions of the transverse field near the neutral line (loci of nulls in the line-of-sight magnetic field which separate opposite-polarity areas) will indicate the orientation of field loops which connect footpoints on opposite sides of the neutral line. During the period of SMM operations, February 1980 to November 1980, the Marshall Space Flight Center (MSFC) magnetograph, which measures the transverse as well as the line-of-sight component of the photospheric field, obtained observations of several flare-productive active regions in which evidence for sheared fields clearly existed.

One of these is the April 1980 region, AR 2372, shown in Figure 1, that was cited above as an example of a rapidly-growing region with attendant spot motions that produced several major flares. In Figure 2, the sunspot movements, which were documented by the Yunnan observations on the 5th, are seen to continue through the 6th, as inferred from the magnetic field changes. From the 5th to the 6th, the isolated positive-polarity spot moved westward toward the large, leading-polarity (positive) spot at $\approx$ 160 ms^{-1}, while the adjacent negative area to the north moved eastward toward the large, following-polarity spot at $\approx$60 ms^{-1}. These motions continued until 1400 UT on the 7th, whereafter no significant motions were observed. The period of spot motion was characterized by frequent and large flares which were centered in the area of these motions. This can be seen in Figure 3 which shows the first large flare on the 5th, and the most intense one, on the 6th.

Evidence that these spot motions produced shear in the magnetic fields of this region is provided by the observed orientations of the transverse fields as shown in Figure 4. At 1407 UT on April 5 (shortly before the flare shown in Fig. 3), the transverse field east of the isolated positive spot was oriented perpendicular across the neutral line. However, to the north and west of this spot, some alignment with

the neutral line is seen implying the presence of shear in the field. By 2055 UT on the 6th, during the period of spot motion, the strong transverse fields are sheared along most of the neutral line, indicative of significant energy storage. Following cessation of spot motion, the shear in the transverse field was less pronounced as observed on the 7th at 1910 UT. Following this apparent relaxation of the field, the high frequency of flares which occurred through the 7th ceased, and little significant flaring was produced on the 8th and 9th.

In an extensive study of these data, Krall et al. [5] estimated the magnetic-energy buildup produced by the relative spot motions to be $\approx 5 \times 10^{32} \times \sin \phi$ erg day^{-1}, where ϕ represents the orientation of the transverse field across the neutral line. This result indicates that there was sufficient energy buildup in the sheared fields to account for the energy released in all the flares that were observed. Using the transverse field data, Krall et al. also calculated the distribution of vertical currents in the area of flare activity. The results were consistent with currents flowing parallel to magnetic loops with footpoints on either side of the neutral line, a configuration which enhances energy-storage capacity [6]. In summary, then, this active region provides ample evidence for energy buildup through the shearing of magnetic loops.

Stressing of magnetic loops may not always be presaged by observed sunspot motions. Complex (i.e., sheared) magnetic configurations can occur as a result of newly-emerged flux which also may produce ""kinky"" neutral lines, satellite spots, δ-configurations, etc. In fact, the presence of a δ-configuration (umbrae of opposite polarity within the same penumbra) has long been recognized as correlating positively with the frequent occurrence of large flares. To examine the physical mechanisms which might be operative in the production of flares within δ-regions, Patty [7] has studied the vector magnetic field structure of δ-regions which were classified as "active" (flare producers) and "non-active" (no significant flare production). In Figure 5, the magnetic field components of active and inactive δ-regions are compared and the results of this investigation are summarized in Table 1, indicating that a combination of strong longitudinal (line-of-sight) gradients with a strong, sheared transverse field is the signature of "active" δ-regions. Again the dominant factor is the presence of shear: non-sheared δ's produce little flare activity. The related signature of steep longitudinal gradients and strong transverse fields may result from the shear, according to the model of Wu et al. [8] in which the shearing of magnetic loops produces a lowering of the field lines and thus a stronger transverse component at the photosphere.

B. Energy Release

Flare-energy release may be triggered by changes in the magnetic field, for example, by further shearing of the fields into unstable configurations or by emergence of new flux. Field changes should also occur as a result of the flare event through field relaxation into less stressed patterns or flux decrease as a result of field annihilation. In this section, we review recent evidence for photospheric field changes which are the direct result of a solar flare occurrence. These changes will be classified as permanent (i.e., they persist after the flare occurs) and transient (appearing and disappearing during the flare).

1. Permanent Changes

Active region (Boulder number) 2456, which was on the solar disk May 14-26, 1980, was selected as a target-region for the SMY Flare Buildup Study. Consequently the region was well observed prior to the two-ribbon flare (2B/X1) on May 21 at 2054 UT. Magnetic field observations provide direct evidence that the field was stressed prior to the flare and that the flare was probably initiated by emerging flux in the center of the active region with subsequent field cancellation occurring [9].

The preflare magnetic field configuration was characterized by an unusual north-south orientation of the leading and following polarities, respectively. The differential rotation of the flux patterns was also unusual with the leading (negative) flux rotating apparently at a faster rate than the equatorial rotation rate. This motion was reflected in the relative sunspot motions during May 18-23 which showed the leading and trailing sunspots separating at ≈ 80 ms^{-1} according to Harvey [9]. It seems reasonable that the magnetic fields were undergoing increasing stress due to this stretching of interconnecting field lines.

Further amplification of field stress probably occurred just prior to the flare with the doubling of the westward velocity of spot "C" relative to the large spots as shown in Figure 6. Also in Figure 6, one can see that two regions of negative flux and a patch of positive flux emerged near the neutral line in the central portion of the active region. This new flux appeared about 80 min before the flare and increased steadily in strength. The configuration of the emerging flux was such that it cancelled existing fields in the region, producing a new flux decrease which is evident in Figure 7. These data are consistent with a bipolar region emerging near the neutral line with an orientation in polarity reversed from that of the main fields and with a field strength sufficient to reverse the strong active region field near the neutral line and weaken it in other areas.

About 2 hr before the flare, the filament (Fig. 8) which outlined the neutral line became active at its west end and developed a kink near its middle section. These changes are presumed to be related to the westward-moving flux near the west end of the filament and the emerging flux beneath its central part. Two hours later the flare erupted (Fig. 9) and, according to Harvey, the total scenario is consistent with the flare model of Kuperus and Van Tend [10]. In their model, photospheric motions create a strongly sheared field that produces the filament turbulence. The appearance of new flux of opposite polarity then increases the filament current leading to the upward motion and eventual eruption of the filament.

In a detailed study of a flare in AR 2372 on April 10, 1980 ($\approx$1725 UT), Moore et al. [11] indicate the flare was triggered by emerging flux associated with a satellite sunspot, and provide evidence that observable changes in photospheric magnetic structure resulted from the flare event. In Figure 10, the preflare situation is shown with the small satellite spot(s) indicated; a penumbral bridge connects the satellite to the larger spot. In Figure 11a, the impulsive onset of the flare is seen in H-alpha -0.8 Å with the brightest emission occurring over the satellite spot. In the following panels, 11b-11e, the flare emission progressed westward towards the filament which subsequently "exploded" in synchrony with the main peak of the impulsive phase. Comparison of Kitt Peak magnetograms before and after the flare, Figures 12 and 13, shows an increase in the magnetic flux associated with the satellite spot. Since Kitt Peak dopplergrams show a strong, blue-shifted feature near the satellite spot, it was concluded that the satellite spot was one "end" of an emerging bipole. Other permanent changes in the magnetic field were inferred from the

disappearance of the penumbral bridge to the companion spot and a truncation of part of the larger spot's umbra. The truncation of the umbra accompanied a local permanent decrease in magnetic flux in the Kitt Peak magnetograms. These subtle photospheric magnetic changes are interpreted to have been wrought by the flare through the strong magnetic change above the photosphere evidenced by the filament eruption.

Permanent weakenings of satellite sunspot fields in flare regions have been observed by Patterson and Zirin [12] using the Big Bear Solar Observatory's videomagnetograph. During two large flares on November 5, 1979, these changes were observed to occur near flare maximum in both cases. In Figure 14, observations for the first flare, which peaked at 2149 UT, are shown. The negative polarity of the satellite field is definitely weakened in the area of densest flare emission, indicated by the HeI D_3 data. The permanent nature of this weakening, which occurred between 2147 and 2149, is confirmed by the magnetogram at 2346 in Figure 15 which was taken prior to the second explosive flare starting at 2347. Further weakening of the satellite field took place during this second flare, again near the area of D_3 emission. The coincidence of these changes with both the time of flare maxima and the locus of maximum intensity seems to provide indisputable evidence that they were flare related. In each flare, magnetic energy on the order of 10^{31} erg could be derived from the observed field weakenings.

To summarize these results, it appears we have new evidence of magnetic field changes before and during flares. The rather subtle nature of these changes may be their most interesting feature since it implies no major photospheric field reorientations need be invoked to trigger or fuel the observed flares.

2. Magnetic Transients

If sudden magnetic field changes occur during flares but disappear very quickly, most magnetograph systems which were in operation during SMY would not record such an event. However, the videomagnetograph at the Big Bear Solar Observatory operates at a sufficiently rapid cadence that magnetic transients, if they do occur, should be observed by that instrument. In fact, several such transient events have been reported by Patterson and Zirin [12] and Zirin and Tanaka [13]. In Figure 16, one of the more striking examples of a transient field change during a flare is shown for the July 1, 1980, flare. The very obvious correlation of the transients with the D_3 emission suggests, however, that the transient might be an artifact produced by emission in the magnetically-sensitive absorption line of FeI at λ5324 which is used in the Big Bear magnetograph. In a recent communication, Zirin indicated that magnetic transients in flares could be explained by the magnetograph line going into emission, but only if the line is narrow ($\lesssim$0.08 Å wide), the emission is approximately twice the background continuum intensity, and the field in the flaring region is concentrated in less than one half the area (i.e., a filling factor greater than 2).

Based on these considerations, it is probable that most of the observed transients are caused by the emission reversal and are not real. However, some transients have been observed in areas not covered by D_3 emission and may therefore be real field changes. It is apparent that we do not have the final answer yet on these interesting observations.

III. MAGNETIC FIELDS AND THE SUNSPOT PHENOMENON

Parker [14] has succinctly described the frustration presented to solar physicists by the sunspot phenomenon when he wrote: "Sunspots are too unstable to form, and, if once formed, should immediately break apart . . . there is much we do not understand." Recent observations and studies of sunspot magnetic fields may have alleviated this frustration somewhat in providing us a better understanding of the three-dimensional morphology of the sunspot field. On the other hand, other recent results indicate that sunspots disappear in a way not yet understood (Liggett and Zirin [15]). Aspects of both these "advances" in our knowledge of sunspots will be discussed in this review.

A. The Sunspot Field

The advent of vector magnetograph observations has allowed measurements of transverse fields in sunspots. This in turn provides quantitative knowledge of the vector-field orientation, specifically the angle Ψ to the line-of-sight and the transverse azimuth ϕ, as well as the field magnitude. Such measurements for simple, long-lived sunspots provide important boundary conditions for magnetohydrostatic models of sunspots.

This approach was used in recent studies by Skumanich and Osherovich [16] and Flaa et al. [17] using observations of sunspot vector fields obtained with the High Altitude Observatory's (HAO) Stokes polarimeter. Using field magnitudes, sunspot geometry and pressure deficits derived observationally, they obtained self-consistent magnetic field, pressure, and temperature distributions based on the return-flux model of Osherovich [18]. One new result from this model is the semi-closed field topology in which the outer (penumbral) field lines return to the photosphere, as seen in Figure 17; the umbral fields remain open as in earlier models. At the umbral-penumbral boundary ($r/r_p = 0.4$ in Fig. 18), the model predicts a field inclination of 25 deg; the inclination at the photospheric boundary ($r/r_p = 1.0$) is 90 deg.

This interpretation of sunspot geometry has been given observational support with the magnetic field observations of Giovanelli [19]; in this study, he has expanded the observational techniques for measurements of network magnetic canopies (Giovanelli, [20]) to those extending from the outer penumbral edge of sunspots. By examination of off-disk-center magnetograms obtained in lines formed at different atmospheric heights, regions at penumbral edges are identified where the diffuse fields at the higher levels extend over field-free regions in the photosphere. From the measured diffuse-field magnitudes, the height of the diffuse field or "canopy," is determined from radiative transfer calculations for a field distribution which is zero below the canopy height Z_0, and uniform and horizontal above Z_0. In a preliminary study of a small super-penumbra, Giovanelli and Jones [21] were able to place a lower limit on the height of the base of the penumbra at its outer edge, using Kitt Peak magnetograph data in the CaII 8542 and FeI 8688 lines. In Figure 19, the Kitt Peak magnetograph data are shown along with a Big Bear Solar Observatory H-alpha photograph which identifies the superpenumbral region. In Figure 20, the derived canopy heights Z_0 are shown at various distances from the penumbral edge. In a continuation of this study, Giovanelli [19] conducted a series of sunspot observations at Kitt Peak.

Using similar techniques, he derived average heights of the magnetic canopy extending from the 14 sunspots which were observed; these results are shown in Figure 21. From this curve, one derives a canopy base angle of 0.5 deg; i.e., the field is almost horizontal. In this same study, Giovanelli made comparisons between measurements of the Wilson depression from limb-side and disk-side penumbral widths; from these he concluded that at the umbral boundary the penumbra is inclined 30 deg to 35 deg from the vertical. Thus, if the penumbral surface defines the field lines, these results are consistent with those of Skumanich and Osherovich [16] in which the field inclination was 25 deg and 0 deg at the umbral and penumbral boundaries, respectively.

A further implication of Giovanelli's results is that the outer portion of the penumbra is elevated $\approx$180 km above the photosphere; Moore [22] has provided evidence of this from high-resolution sunspot photographs which indicate that dark penumbral filaments overlie bright granules in certain areas.

From this work by Giovanelli and others, a new picture of the horizontal penumbral field forming a low canopy over the photosphere is obtained. Turning now to the vertical extension of sunspot fields, a long-standing problem has been the extent to which these fields penetrate into the higher levels of the solar atmosphere. To address this, a collaborative investigation was undertaken during the Solar Maximum Mission to obtain co-temporal measurements of a sunspot's magnetic field at photospheric and transition-region levels. The photospheric sunspot field was measured in all three components with the NASA, Marshall Space Flight Center (MSFC) vector magnetograph (Hagyard et al., [23]). The line-of-sight component of the field in the transition region was measured using the Ultraviolet Spectrometer and Polarimeter (UVSP) instrument (onboard the SMM satellite) operating in a magnetograph mode (Tandberg-Hanssen et al. [24]). In Figure 22, the observed sunspot is shown together with an MSFC magnetogram and spot intensity contours showing the position of the UVSP raster relative to the sunspot. From the two data sets, line-of-sight fields were derived for the photosphere and transition region as shown in Figure 23. To extrapolate the photospheric field in the vertical direction for comparisons with the transition-region (UVSP) fields, a potential calculation was performed using the MSFC line-of-sight data as boundary values. In Figure 24, the variation of the potential line-of-sight field with height is shown for the four UVSP raster pixels which covered the large umbral region (pixels 4, 10, 11, 17). From these curves it was determined that the extrapolated potential (line-of-sight) field matched the UVSP data at heights ranging from 3800 to 8100 km, yielding the vertical gradients shown in Table 2. These results were compared with vertical gradients calculated from the condition $\nabla \cdot \underset{\sim}{B} = 0$, using the observed transverse field; the comparisons were favorable. Based on this and the agreement noted between the observed transverse field and that derived from the potential calculation at $z = 0$, it was concluded that the field of this sunspot was well represented by a potential distribution. Consequently, from these analyses it seems that the vertical gradient of the line-of-sight component is lower than values from previous studies and the transition region field occurs at an average height of $\approx$ 6500 km above the photosphere (Hagyard et al. [25]).

Recently, Akhmedov and collaborators [26] from the Pulkovo Observatory in Russia have measured magnetic fields above umbral regions in sunspots using solar radio emission in the 2.0 to 4.0 cm wavelength range. Their measurements, which were obtained with the RATAN-600 radio telescope, are based on the interpretation of the radio data in terms of gyroresonance emission. By determining the shortest wavelength at which circular polarization is detected, the maximum magnetic field at

a height of ≈2000 km above the umbral area was determined with ≈17 arc sec resolutio Comparisons of these field intensities with fields corresponding to the photospheric umbra gave field gradients of ≈ 0.25 G km^{-1} and field decreases of 10 to 20 percent. These results are consistent with those cited from the previous study (Hagyard et al. [25]) and again indicate that the umbral fields extend into the solar corona with 1 to 2 kG intensities.

In concluding this section, it is well to keep in mind the careful work being done by Zwaan and his colleagues (Brants and Zwaan [27]) in measurements of field strengths in sunspot umbrae. Their results remind us of the ever-present danger of scattered light and its effect on the interpretation of field strengths in sunspots, especially the smaller ones.

Scattered light is not the only problem in sunspot magnetic field measurements. Landi Degl'Innocenti [28] and Landolfi and Landi Degl 'Innocenti [29] have shown that magneto-optical effects must be considered in interpretations of vector magnetograph data. In a recently-completed study, West and Hagyard [30] have indeed shown that the transverse field azimuth direction is rotated anomalously, presumably by Faraday rotation. In Figure 25, they show the observed azimuth angles (points) at different spectral positions within the FeI 5250 Å absorption line; these observed angles deviate considerably from the expected azimuth orientations (dashed curve). If the field azimuth were rotated by Faraday rotation, the observed azimuth would vary with wavelengths as indicated by the solid curves. Apparently, these results confirm the presence of Faraday rotation in sunspot observations and warn us that care must be exercised in the interpretation of measurements of linear polarization.

B. Demise of a Sunspot

We have seen that recent research on the three-dimensional morphology of well-developed sunspots has given us some intriguing new results concerning umbral and penumbral field distributions. What happens to these fields as a sunspot "dies" turns out to be an equally intriguing phenomenon based on recent research at the Mount Wilson and Big Bear observatories.

1. Now You See It

From observations at the Potsdam Tower Telescope (Kunzel [31]) made at a 30-min cadence over a 2-day period, it appears that umbral field strengths of a well-developed sunspot region vary very little over this time period. In Figure 26, the measured field strength is shown for September 3-4, 1980, for the leading umbral region which appeared to undergo no apparent morphological changes over the time-span of September 2-5, based on white-light sunspot photographs.

But it is known that the process of sunspot dissolution begins soon after the formation and stabilization of such a sunspot group, so that one expects to see some characteristic decline or dissolution of these strong umbral fields as the spots decay. The nature of this field decline is the subject of this section.

2. Now You Don't

In a recent study, Mount Wilson observations of 25 sunspots which disappeared near central meridian were examined by Wallenhorst and Howard [32]. They evaluated the magnetic flux of the entire active region associated with the disappearing spot

and plotted both positive and negative flux as a function of time, with time zero taken as the day of spot disappearance. Their results are shown in Figure 27 with active regions of higher flux appearing toward the top of the figure. In 23 out of 25 events, the flux decreases on or shortly after the day of spot disappearance. In Figure 28, the average total flux for all 25 cases is shown as well as the non-active region ("background") flux. The average individual spot flux was $\approx 0.5 \times 10^{20}$ Mx whereas the average active-region flux decrease was $\approx 12 \times 10^{20}$ Mx as shown in this figure. Since the non-active region flux remains almost constant, Wallenhorst and Howard concluded that the spot field did not diffuse into the background field but, in fact, disappeared!

To further investigate this result, a collaborative investigation was undertaken by the Mount Wilson and Big Bear solar observatories. In this coordinated observing program, Wallenhorst and Topka [33] observed a small sunspot group during June 16-20, 1981, through the time of sunspot disappearance on June 19. Videomagnetograms and H-alpha photographs were obtained from Big Bear, and the Mount Wilson Babcock magnetograph provided daily finescans of the region. In Figure 29, the Mount Wilson data are shown for each day in the interval June 16-20; in Figure 30, the measured negative flux is shown together with the background flux. From these data, it was concluded that there was a real flux decrease which was not caused by the field spreading out into the background nor by large-scale, low-lying reconnection. The spot flux of $\approx 8 \times 10^{20}$ Mx was again less than the flux decrease of $\approx 20 \times 10^{20}$ Mx.

The Big Bear observations were able to isolate the sunspot polarity and follow its decay, primarily because of the moat which initially surrounded the spot as shown in Figure 31. The Big Bear observations also show the appearance of a supergranule on the 17th which coincided with the gradual disintegration of the spot field by the breaking off of magnetic knots which then moved away from the spot with a direction and velocity determined by the supergranular flows. On the 19th, the remnant spot polarity was swept to the edge of the supergranulation cell and disappeared.

The Big Bear observations reinforced the conclusions derived from the Mount Wilson data. Moreover, they suggest that the sunspot field disappears by fragmentation and redistribution caused by supergranular flows but the flux of the entire active region decreases by a steady removal of flux from the photosphere with no evidence for the field spreading into the background field. They suggest a flux removal mechanism which does not require flux cancellation at the neutral line since flux disappearance is seen to occur for elements well removed from the neutral line.

3. Naked Sunspots

Liggett and Zirin [15] have come up with the titillating title of "naked sunspots" to describe a class of sunspots which are devoid of associated plage and have little or no associated opposite-polarity fields, as can be seen in Figure 32. These spots are long-lived remnants of sunspot groups which had a large, symmetric "p" spot. As Liggett and Zirin point out, when one of these naked spots disappears, nothing remains — no remnant plage, no field. Clearly, removal of flux from the photosphere occurs during the process, but, of course, the unanswered question is how? The death of a sunspot is as puzzling as the sunspot phenomenon itself.

IV. FIELDS OUTSIDE ACTIVE REGIONS

In this section, new results are discussed concerning magnetic features which are generally not associated with solar activity: network fields, turbulent magnetic flux, and polar crown prominences. Recent developments concerning the solar magnetic cycle will be discussed in the final section.

A. Network Canopies

The kilogauss fields that are concentrated in sub-arc second elements along supergranule boundaries can be contained only at depths where the external gas pressure is sufficient to maintain pressure balance. Above the photosphere, where the gas pressure falls off rapidly, the flux tubes must fan out, forming a "canopy" over the nearly non-magnetic interior of the network, as shown schematically in Figure 33 (Giovanelli [20]). The height Z_0 of this approximately horizontal canopy was given as 1500 km by Gabriel [34].

Magnetograph data from lines formed at different atmospheric levels provide evidence for these canopies. First, network fields of individual supergranular cells in active regions near the limb, which are unipolar in photospheric magnetograms, appear bipolar with a limbward reverse polarity in magnetograms from lines formed above the photosphere. Interpreting this observation on the basis of Figure 33, Zeeman-sensitive lines formed at $\tau_c = 1$ (well below the canopy base at Z_0) will produce the unipolar network, whereas those formed near Z_0 will reflect the opening out of the field lines through polarity reversals across the supergranule. A further magnetograph manifestation of network canopies comes from the observed diffuse extension of higher fields over regions which are field-free at the photosphere.

Using Kitt Peak magnetograms in the FeI 5233 and MgI b_2 5173 lines, Giovanelli [20] investigated these network magnetic characteristics to derive the height and extent of network canopies; his technique was similar to that used for penumbral canopies as described in Section III.A. What he found was that, in well-developed networks, the canopy base was only 500 to 600 km above $\tau_c = 1$, much lower than previously accepted. Based on this result and the measured extent of the canopy base ($\approx 10^4$ km), Giovanelli inferred the "typical" network field configuration shown in Figure 34. Such a field morphology has significant implications for a number of solar features such as H-alpha fibrils, the chromosphere-corona transition region, wave-propagation, and fields derived from potential theory; these are discussed by Giovanelli [20].

B. Turbulent Magnetic Fields

The network canopies described above are formed from the opening outwards of the concentrated kilogauss fields at supergranular boundaries. As indicated by Stenflo [35], these strong fields reside in only a few tenths of a percent of the solar surface. The remaining approximately 99 percent of the solar surface, over which the network canopies extend, appears to be field-free, but Stenflo argues that this may not be true: a small-scale, inner-network, turbulent magnetic field would be "hidden" because the field is weak and the polarities integrate out within the observational spatial resolution.

Blending once again a thorough comprehension of physical processes with his observational skills, Stenflo [35] has provided initial evidence of an inner-network turbulent magnetic flux. His results are based on observations (near the north and south poles) of the linear Stokes profiles in a number of spectral lines, using the HAO Stokes polarimeter. The measured degree of linear polarization is interpreted on the basis of the Hanle effect which changes the linear polarization caused by coherent scattering when weak magnetic fields are present. By estimating the contributions to the linear polarization from other effects (atomic depolarization, collisional depolarization, scattering geometry, and a non-LTE factor), Stenflo was able to estimate the Hanle depolarization k_H from the observed linear polarization p_o. Since $k_H = k_H(k_c, B_t)$, where k_c is the collisional depolarization and B_t is the weak (turbulent) magnetic field intensity, Stenflo plotted the derived values of k_H versus calculated values of k_c for the observed spectral lines and compared these points with theoretical curves derived for various values of B_t. His results are shown in Figure 35 and indicate that B_t should be stronger than 10 G near the temperature minimum in the solar atmosphere. An upper limit of 100 G is also indicated which agrees with previous results derived from magnetic line broadening (Stenflo and Lindegren [36]).

C. Polar Crown Prominences

In another application of the Hanle effect method, Leroy [37] has measured the magnetic fields in high-latitude prominences. Over the period 1974 to 1980, 120 polar crown prominences were observed to determine the magnitude and direction of linear polarization in the HeI D_3 line with 5 arc sec resolution. From the observed depolarization and rotation of the linear polarization vector, Leroy derived the magnitude B of the field and the angle θ of the magnetic vector with respect to the solar parallel. Two interesting results were derived from analyses of these data, concerning the orientation of the transverse field in prominences and the cyclic reversal of the axial prominence field.

For the polar prominences which were observed exactly edge-on at the limb, the angle α between the prominence's vector field and the long axis of the prominence could be determined unambiguously from the observed θ. For prominences not observed edge-on, the symmetry of θ with respect to the line-of-sight leads to two possible values of α. In analyzing these data, Leroy made two independent determinations of α based on two assumed orientations of the transverse magnetic field in prominences: one consistent with a Kippenhahn-Schluter (KS) configuration [38] and one consistent with the Kuperus-Raadu (KR) model [39]. With the derived α-values, histograms were plotted for (a) the cases where prominences were observed exactly edge-on with α-values independent of models, (b) the set of prominences not observed edge-on with α-values based on the KR model, and (c) the same set as (b) with α-values determined from a KS configuration. These histograms are shown in Figure 36 and indicate the observed prominences had transverse fields consistent with the Kuperus-Raadu model. This result has been confirmed recently for low-latitude quiescent prominences also (Leroy, private communication).

From observations of polar crown prominences during 1964 to 1965, Rust [40] determined that almost all northern polar crown prominences had the same orientation of polarity in the axial fields, and inferred from observations of southern polar

prominences that this was a cyclic phenomenon which would produce reversed polarities in the following cycle. From measurements of field directions in prominences during the period of polar field reversal for the current solar cycle, Leroy obtained direct evidence for the dependence of field polarities in prominences on the polarity of the surrounding high-latitude photospheric fields. In Figure 37, the photospheric fields and prominence field directions are shown schematically for the prominences on the solar surface on July 15, 1980. Remnants of the old polarity fields exist at the poles along with polar crown prominences whose magnetic vectors are oriented in directions similar to those prominences occurring prior to solar maximum. Yet the field vector in prominences observed at lower latitudes is reversed, reflecting the reversal of the surrounding photospheric fields. Thus, we are observing the transitional period in the cyclic change of solar prominence fields.

V. THE SOLAR MAGNETIC CYCLE

The cyclic change in axial directions of the magnetic field of polar crown prominences is just one aspect of the solar magnetic cycle which solar physicists have attempted to understand and model for many years. Now, as a result of comprehensive analyses of Mount Wilson synoptic data, two phenomena have recently been discovered which certainly must play significant roles in that cycle.

A. Emerging Flux and Torsional Oscillations

From studies of full-disk velocity data obtained at Mount Wilson over a 13-year period, Howard and LaBonte [41] discovered the presence of torsional oscillations on the Sun. In a further study (LaBonte and Howard [42], they presented arguments that these motions are a manifestation of a fundamental oscillation within the Sun that is responsible for the solar magnetic cycle. Specifically, from analyses of the synoptic Mount Wilson magnetic field data, it was discovered that the magnetic fields which form the solar active regions of a magnetic cycle emerge in latitude strips that are centered near the shear zone which is situated between the eastward and westward flows of the torsional oscillations. Moreover, in every case, this zone lies poleward of the westward motions. From this it was argued that the torsional oscillations must slowly amplify subsurface magnetic fields until the fields emerge at the sunspot latitudes. Moreover, the absence of emerging fields at all other shear zones was taken as evidence for the localization of the subsurface magnetic field within the torsional wave: the velocity and magnetic fields, according to LaBonte and Howard [42], are two components of a single wave mode. The authors also argue that the α-ω solar dynamo model predicts a torsional wave which has wave properties that differ from the observed torsional oscillations; hence they indicate that this α-ω model may not be operative in the Sun.

B. Polar Fields and Meridional Flows

Following a re-reduction of Mount Wilson magnetic field data covering an interval of over 13 years, Howard and LaBonte [43] analyzed the global properties of solar magnetic fields. They found that large-scale magnetic fields originate only in the sunspot latitudes, and the polar fields are generated exclusively by isolated episodes of movement of following-polarity fields from the sunspot latitudes to the poles. From the characteristics of this polar transport process, the authors conclude it does not occur by diffusion but as a result of a meridional flow, and they speculate that this flow is the meridional component of a large-scale, subsurface circulation pattern.

Topka et al. [44], using filaments as independent tracers of the poleward flux migration, have confirmed the need for a global poleward flow of order 10 ms^{-1} to produce the observed poleward transport of both the field and the filaments.

These results concerning the solar activity cycle force us to recognize new concepts about that cycle (torsional oscillations and magnetic fields localized within the torsional wave), and to question other concepts (α-ω dynamos, a general dipole solar field). The incorporation of these new findings into a self-consistent model of the Sun's magnetic cycle represents a challenging problem for theorists in the next few years.

VI. CONCLUDING REMARKS

As indicated at the end of the preceding section, while advances in research in solar magnetic fields during the period covered in this review have resolved certain questions, many other provocative questions have arisen for our future consideration, and it is hoped that a primary result of this review will be the stimulation of ideas for new observations and research. And, while the studies undertaken during the SMY did not resolve all our problems, the international collaborations, which originated because of the SMY program, in themselves represent a significant contribution to solar research.

REFERENCES

1. Hong, Q., Ding, Y., and Luan, D.: Acta Astronomia Sinica, Vol. 23, 1982, p. 327.

2. Zirin, H. and Tanaka, K.: Solar Phys., Vol. 32, 1973, p. 173.

3. Tanaka, K. and Nakagawa, Y.: Solar Phys., Vol. 33, 1973, p. 187.

4. Neidig, D. F.: Solar Phys., Vol. 61, 1979, p. 121.

5. Krall, K. R., Smith, J. B., Hagyard, M. J., West, E. A., and Cumings, N. P.: Solar Phys., Vol. 79, 1982, p. 59.

6. Sakurai, T.: Solar Phys., Vol. 69, 1981, p. 343.

7. Patty, S. R.: in Physics of Sunspots, Proceedings of a Workshop, Sunspot, New Mexico, July 1981.

8. Wu, S. T., Hu, Y. Q., Nakagawa, Y., and Tandberg-Hanssen, E.: Astrophys. J., Vol. 266, 1983, p. 866.

9. Harvey, J. W.: In Advances in Space Research, Vol. 2, Proceedings of COSPAR Symposium on the Solar Maximum Year, May 1982, Ottawa, Canada, 1982, p. 31.

10. Kuperus, M. and Van Tend, W.: Solar Phys., Vol. 71, 1981, p. 125.

11. Moore, R. L., Hurford, G. J., Jones, H. P., and Kane, S. R.: Astrophys. J., Vol. 276, 1984, p. 379.

12. Patterson, A. and Zirin, H.: Astrophys. J., Vol. 243, 1981, p. L99.

13. Zirin, H. and Tanaka, K.: Astrophys. J., Vol. 250, 1981, p. 791.

14. Parker, E. N.: Solar Phys., Vol. 40, 1975, p. 291.

15. Liggett, M. and Zirin, H.: Big Bear Solar Observatory Preprint No. 0212, 1982.

16. Skumanich, A. and Osherovich, V. A.: in Physics of Sunspots, Proceedings of a Workshop, Sunspot, New Mexico, July 1981.

17. Flaa, T., Osherovich, V. A., and Skumanich, A.: Astrophys. J., Vol. 261, 1982, p. 700.

18. Osherovich, V. A.: Solar Phys., Vol. 77, 1982, p. 63.

19. Giovanelli, R. G.: Solar Phys., Vol. 80, 1982, p. 21.

20. Giovanelli, R. G.: Solar Phys., Vol. 68, 1980, p. 49.

21. Giovanelli, R. G. and Jones, H. P.: Solar Phys., Vol. 79, 1982, p. 267.

22. Moore, R. L.: Astrophys. J., Vol. 249, 1981, p. 390.

23. Hagyard, M. J., Cumings, N. P., West, E. A., and Smith, J. E.: Solar Phys., Vol. 80, 1982, p. 33.

24. Tandberg-Hanssen, E., Athay, R. G., Beckers, J. M., Brandt, J. C., Bruner, E. C., Chapman, R. D., Cheng, C. C., Gurman, J. B., Henze, W., Hyder, C. L., Michalitsianos, A. G., Shine, R. A., Schoolman, S. A., and Woodgate, B. E.: Astrophys. J., Vol. 244, 1981, p. L127.

25. Hagyard, M. J., Teuber, D., West, E. A., Tandberg-Hanssen, E., Henze, W., Beckers, J. M., Bruner, M., Hyder, C. L., and Woodgate, B. E.: Solar Phys., Vol. 84, 1983, p. 13.

26. Akhmedov, Sh. B., Gelfreikh, G. B., Bogod, V. M., and Korzhavin, A. N.: Solar Phys., Vol. 79, 1982, p. 41.

27. Brants, J. J. and Zwaan, C.: Solar Phys., Vol. 80, 1982, p. 251.

28. Landi Degl'Innocenti, E.: Solar Phys., Vol. 63, 1979, p. 237.

29. Landolfi, M. and Landi Degl'Innocenti, E.: Solar Phys., Vol. 78, 1982, p. 355.

30. West, E. A. and Hagyard, M. J.: Solar Phys., Vol. 88, 1983, p. 51.

31. Kunzel, H.: in Proceedings of the SMY International Workshop, Vol. 2, Simferopol, Crimea, March 1981, p. 266.

32. Wallenhorst, S. G. and Howard, R.: Solar Phys., Vol. 76, 1982, p. 203.

33. Wallenhorst, S. G. and Topka, K. P.: Solar Phys., Vol. 81, 1982, p. 33.

34. Gabriel, A. H.: Phil. Trans. Roy. Soc., Vol. A281, 1976, p. 339.

35. Stenflo, J. O.: Solar Phys, Vol. 80, 1982, p. 209.

36. Stenflo, J. O. and Lindegren, L.: Astron. Astrophys., Vol. 59, 1977, p. 367.

37. Leroy, J. L., Bommier, V., and Sahal-Brechot, S.: Solar Phys., Vol. 83, 1983, p. 135.

38. Kippenhahn, R. and Schluter, A.: Z. Astrophys., Vol. 43, 1957, p. 36.

39. Kuperus, M. and Raadu, M. A.: Astron. Astrophys., Vol. 31, 1974, p. 189.

40. Rust, D. M.: Astrophys. J., Vol. 150, 1967, p. 313.

41. Howard, R. and LaBonte, B. J.: Astrophy. J., Vol. 239, 1980, p. L33.

42. LaBonte, B. J. and Howard, R.: Solar Phys., Vol. 75, 1982, p. 161.

43. Howard, R. and LaBonte, B. J.: Solar Phys., Vol. 74, 1981, p. 131.

44. Topka, K., Moore, R., LaBonte, B. J., and Howard, R.: Solar Phys., Vol. 79, 1982, p. 231.

TABLE 1. SUMMARY OF MAGNETIC CHARACTERISTICS OF δ REGIONS

	Active δ	Inactive δ
Maximum B_L	800 G	300 G
Maximum B_T	1300 G	1000 G
Gradient B_L	0.24 G km^{-1}	0.12 G km^{-1}
ϕ across neutral line	$\approx$ parallel	$\approx$ perpendicular

TABLE 2. POTENTIAL THEORY GRADIENTS IN GAUSS km^{-1}

Pixel	Z* (km)	$\overline{(\Delta B_z/\Delta z)}_{z*}$
4	3800	0.157
10	8100	0.097
11	7300	0.112
17	6600	0.105

*Height at which potential field matches UVSP data.

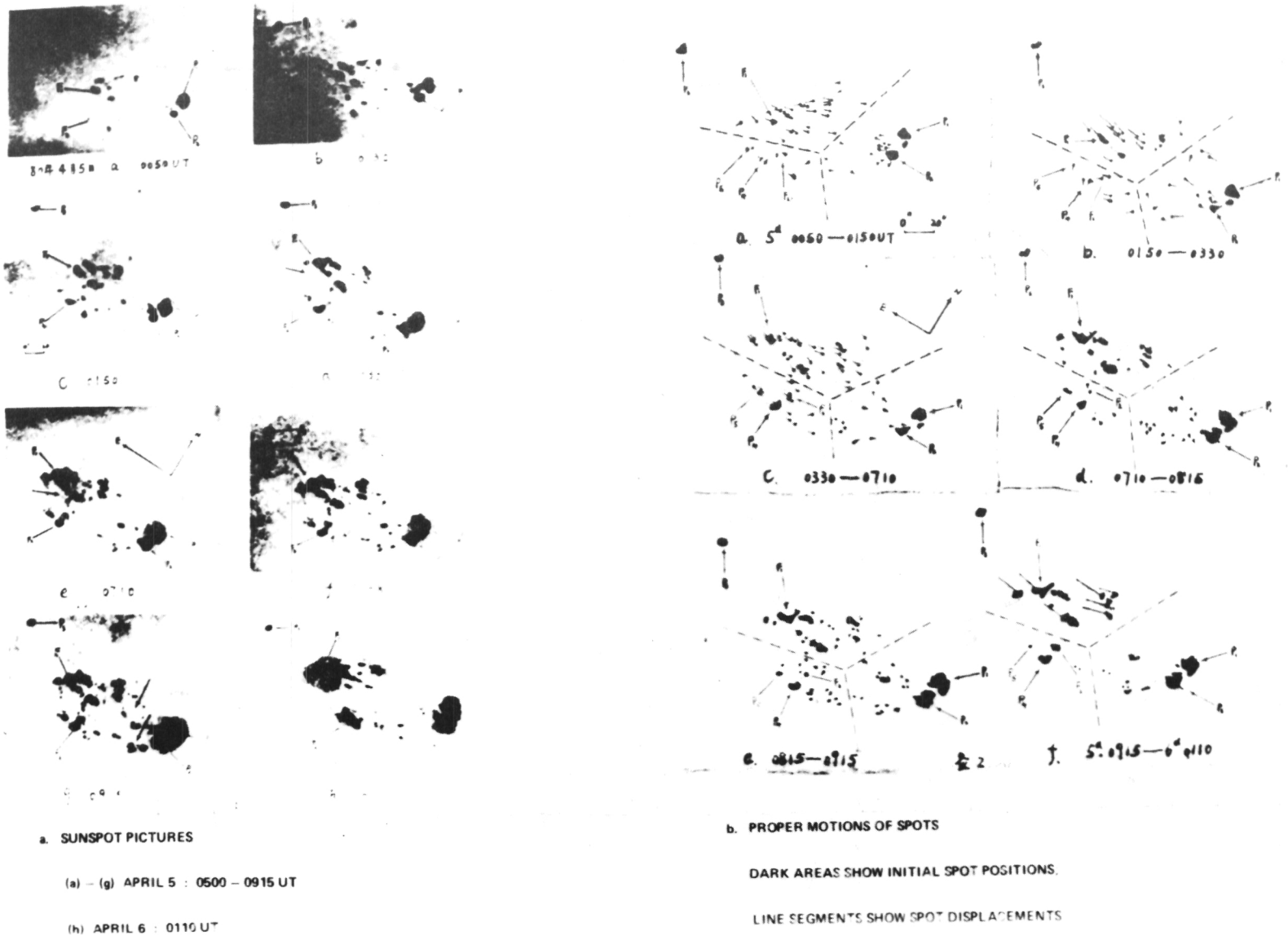

Figure 1. Sunspot pictures and inferred motions from the Yunnan Observatory.

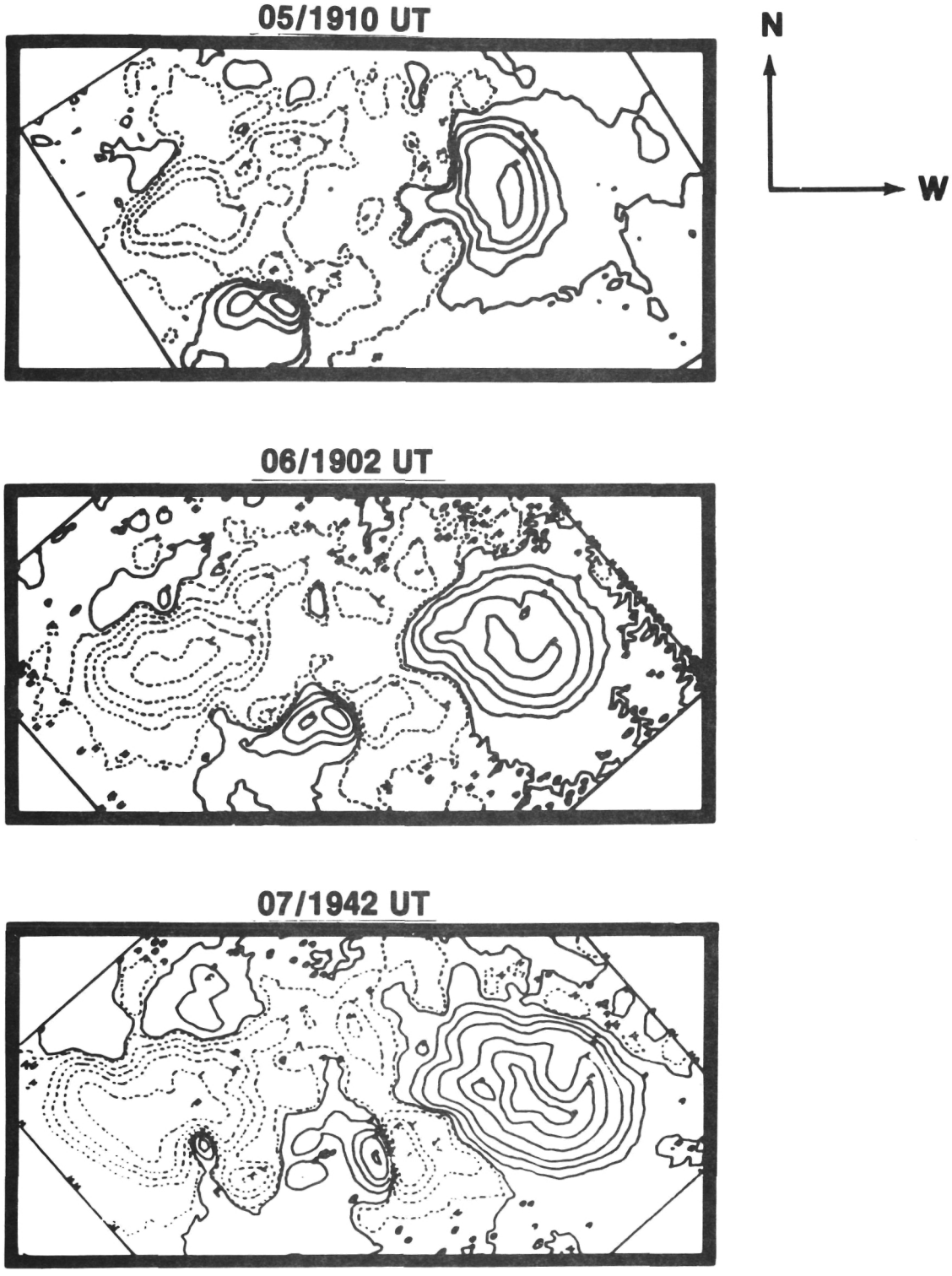

Figure 2. Evolution of the line-of-sight magnetic fields in active region 2372 for the time interval April 5-7.

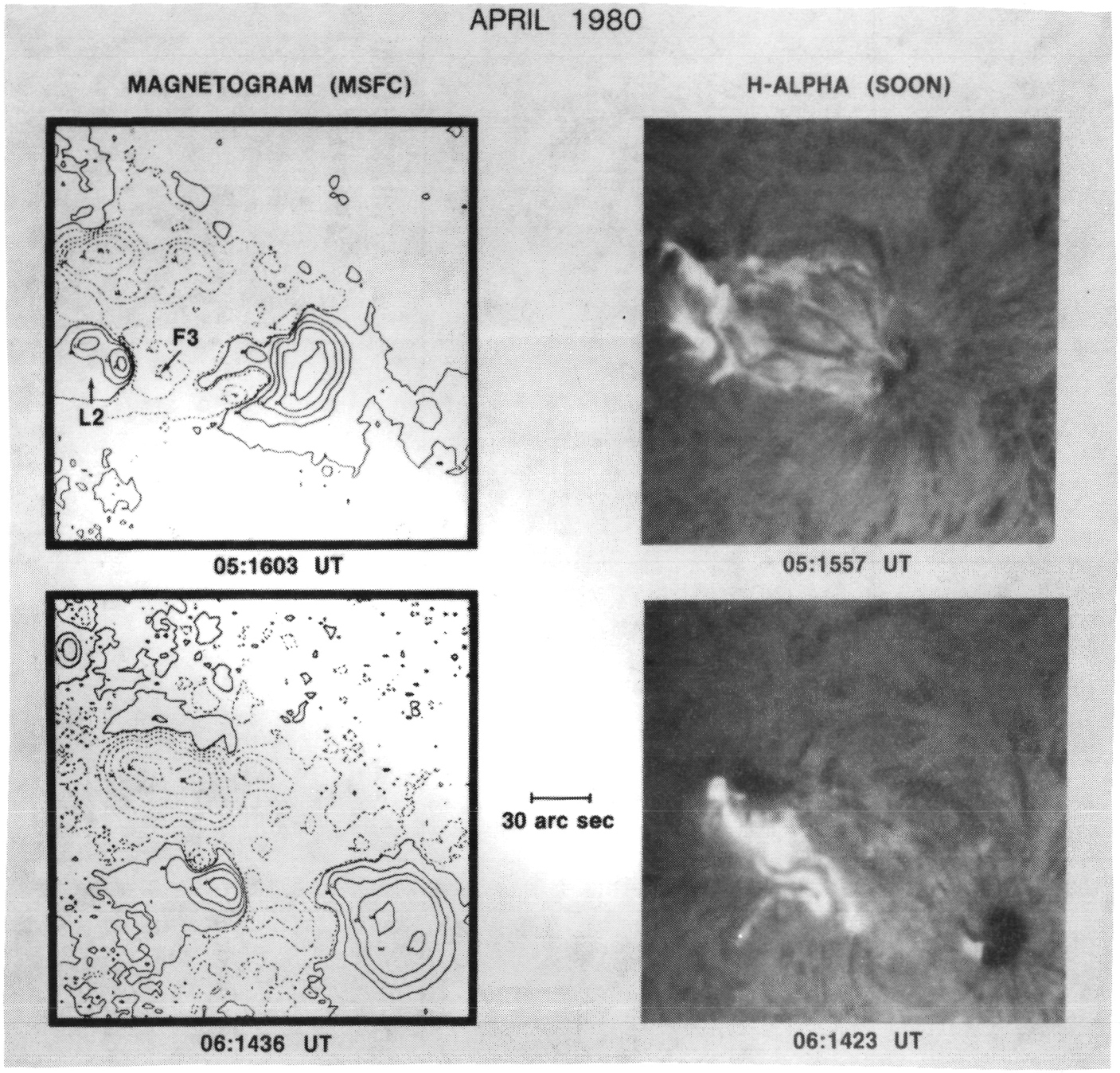

Figure 3. Magnetograms and H-alpha spectroheliograms of active region 2372 at the times of two flares.

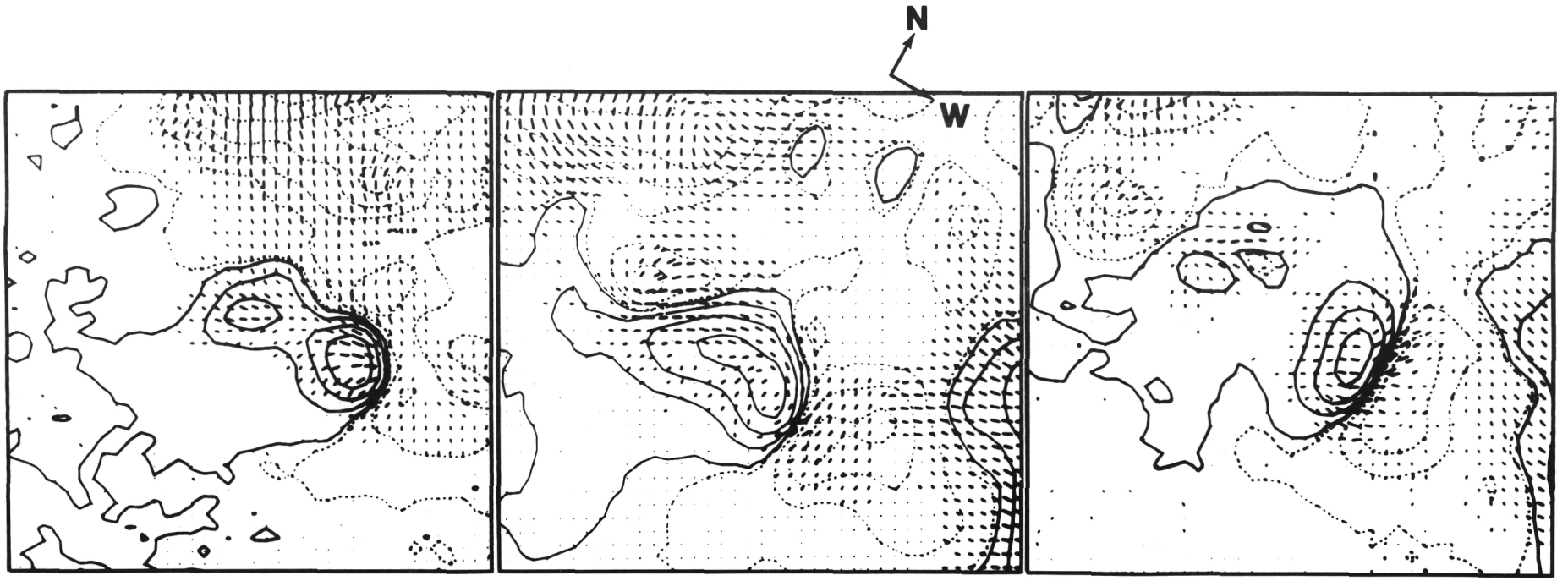

Figure 4. Evolution of the transverse magnetic field of active region 2372 during the interval April 5-7.

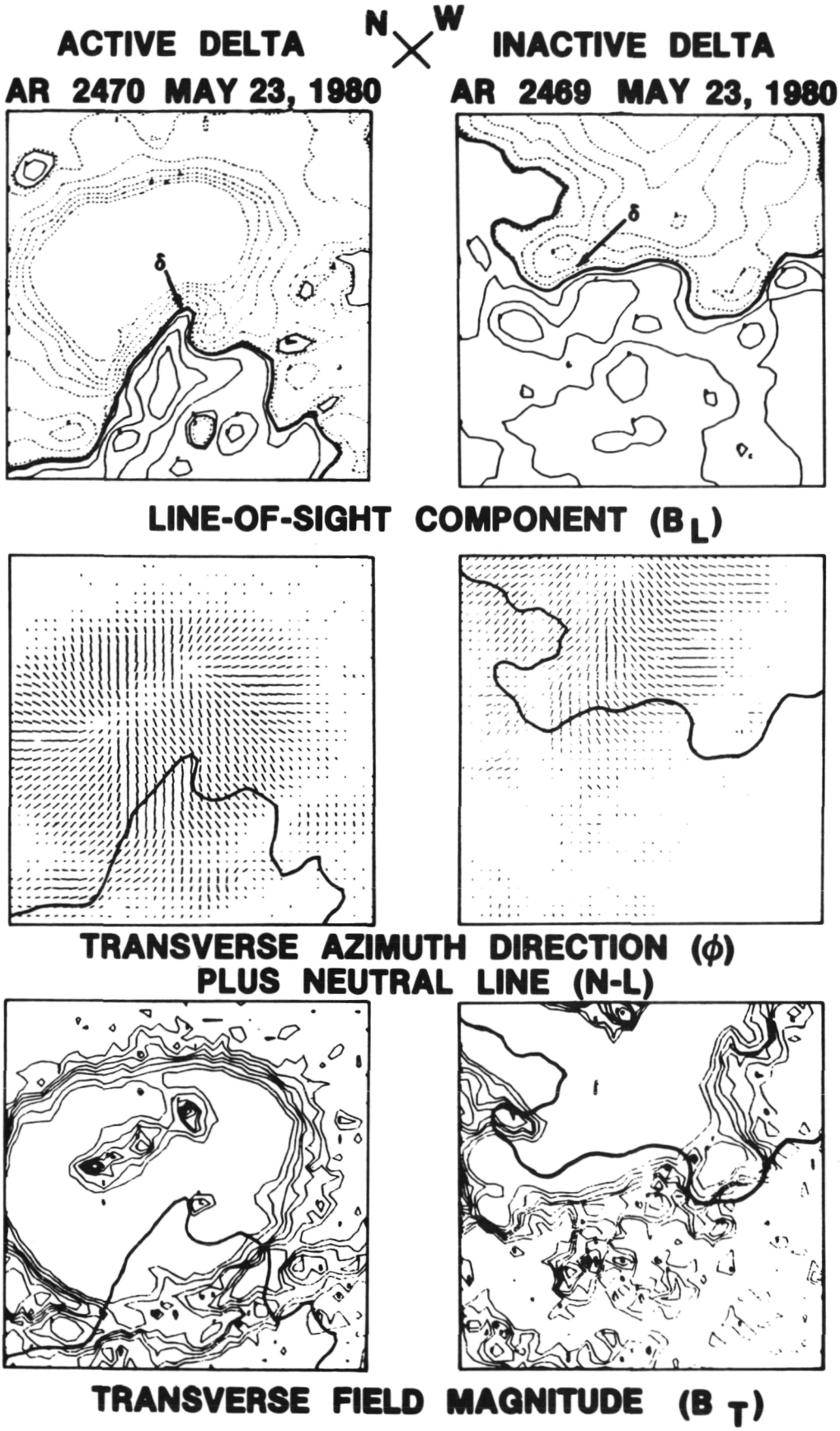

Figure 5. Magnetic fields of "active" and "inactive" delta regions.

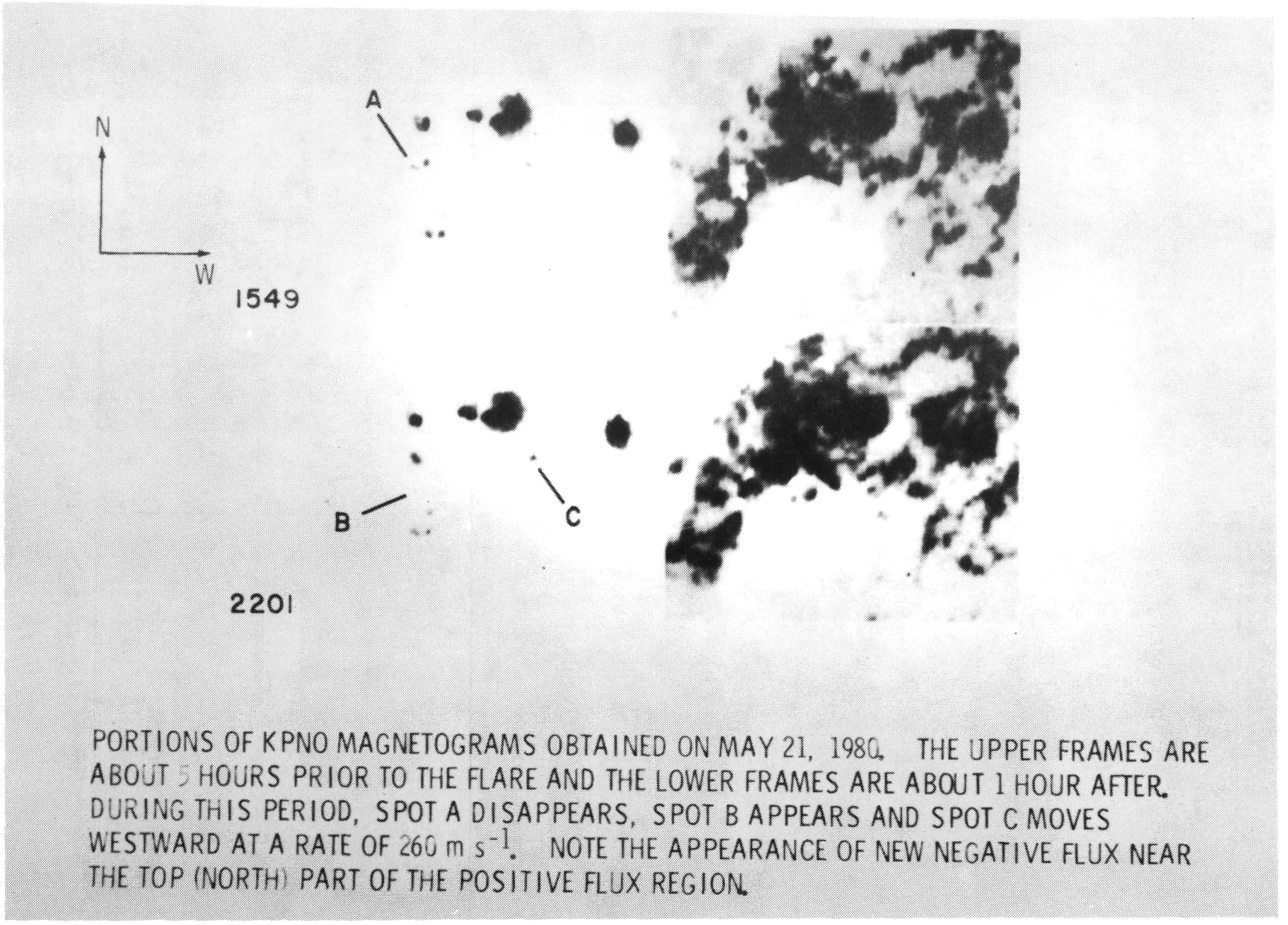

PORTIONS OF KPNO MAGNETOGRAMS OBTAINED ON MAY 21, 1980. THE UPPER FRAMES ARE ABOUT 5 HOURS PRIOR TO THE FLARE AND THE LOWER FRAMES ARE ABOUT 1 HOUR AFTER. DURING THIS PERIOD, SPOT A DISAPPEARS, SPOT B APPEARS AND SPOT C MOVES WESTWARD AT A RATE OF 260 m s^{-1}. NOTE THE APPEARANCE OF NEW NEGATIVE FLUX NEAR THE TOP (NORTH) PART OF THE POSITIVE FLUX REGION.

Figure 6. Longitudinal magnetograms (KPNO) before and after the large flare of May 21, 1980.

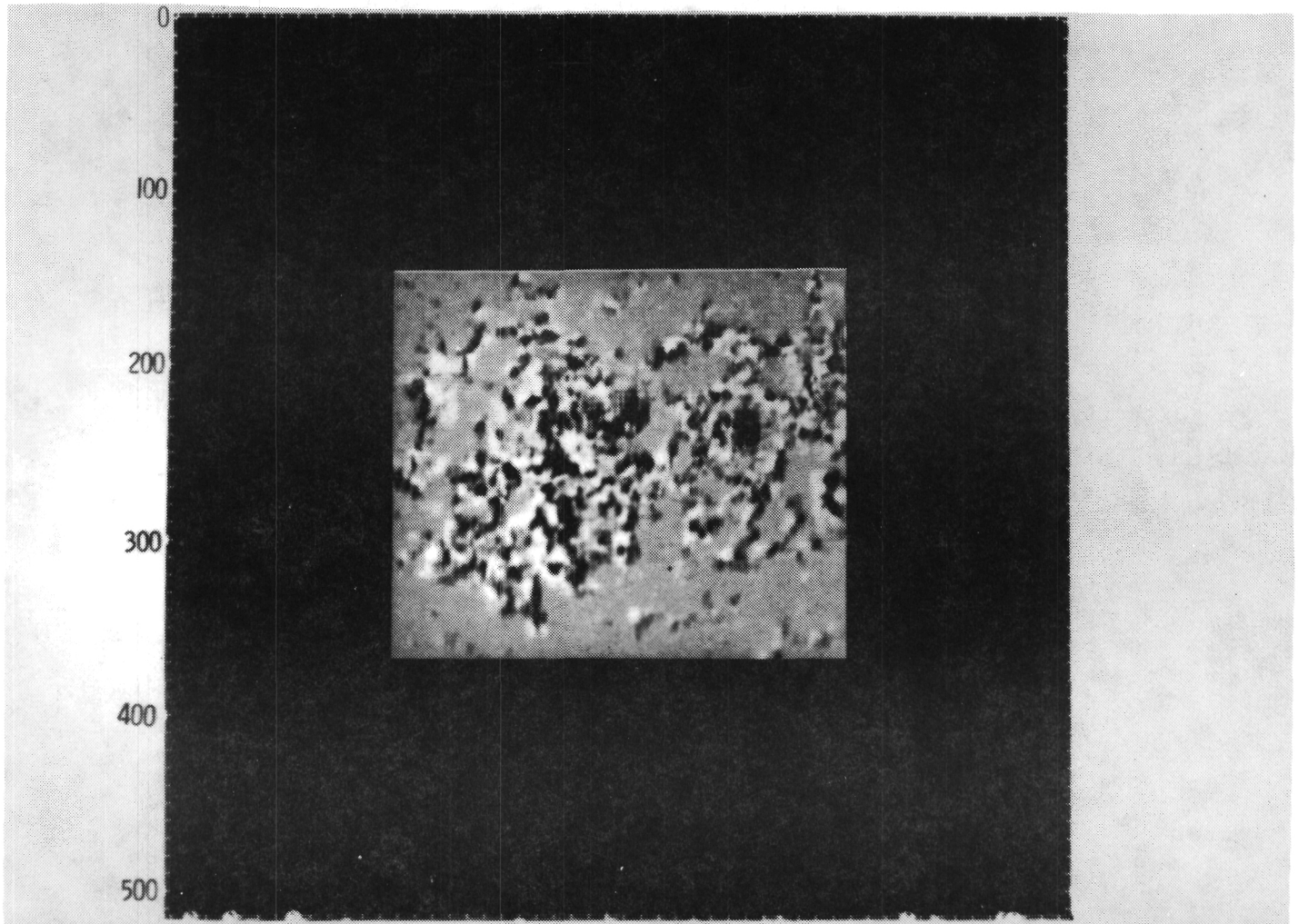

Figure 7. Map of the difference in absolute magnetic flux before and after the flare of May 21, 1980.

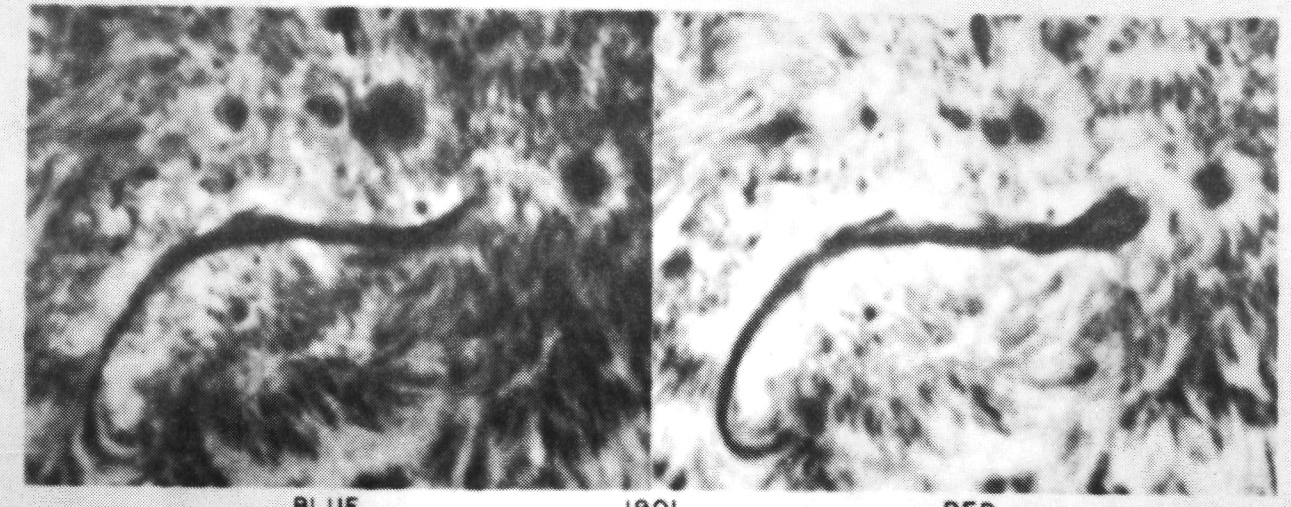

PHOTOGRAPHS IN THE WINGS OF THE Hα LINE MADE AT 1901 UT ON MAY 21, 1980. NORTH IS UP AND WEST IS TO THE RIGHT. NOTE STRONG DOWNFLOW (RED SHIFT) IN THE WESTERN END OF THE FILAMENT. PHOTOGRAPHS FROM HOLLOMAN SOLAR OBSERVATORY, COURTESY OF D. RUST.

Figure 8. Spectroheliograms in the red and blue wings of H-alpha shortly before the flare of May 21, 1980.

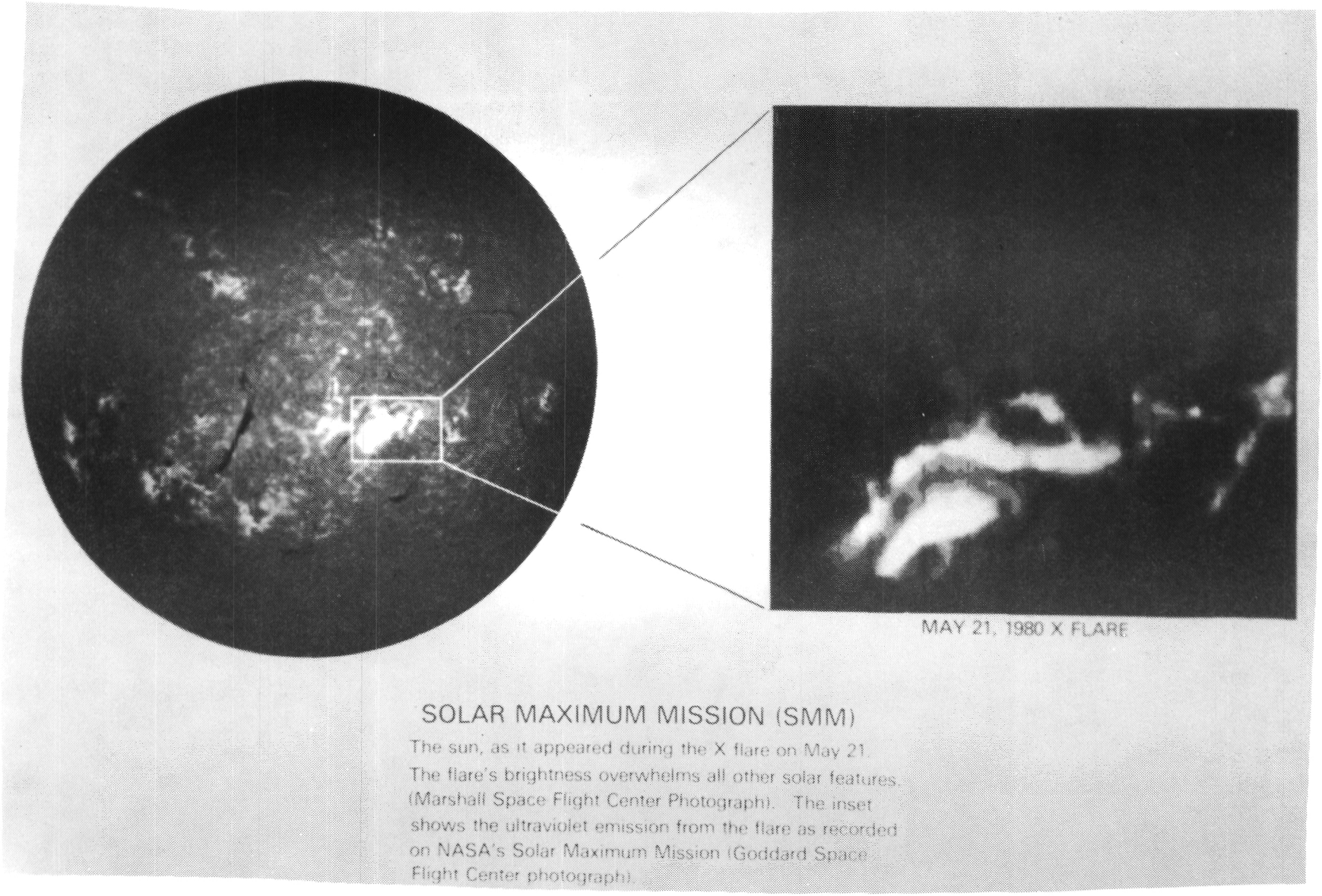

Figure 9. The flare of May 21, 1980, in H-alpha with inset showing the the accompanying ultraviolet emission.

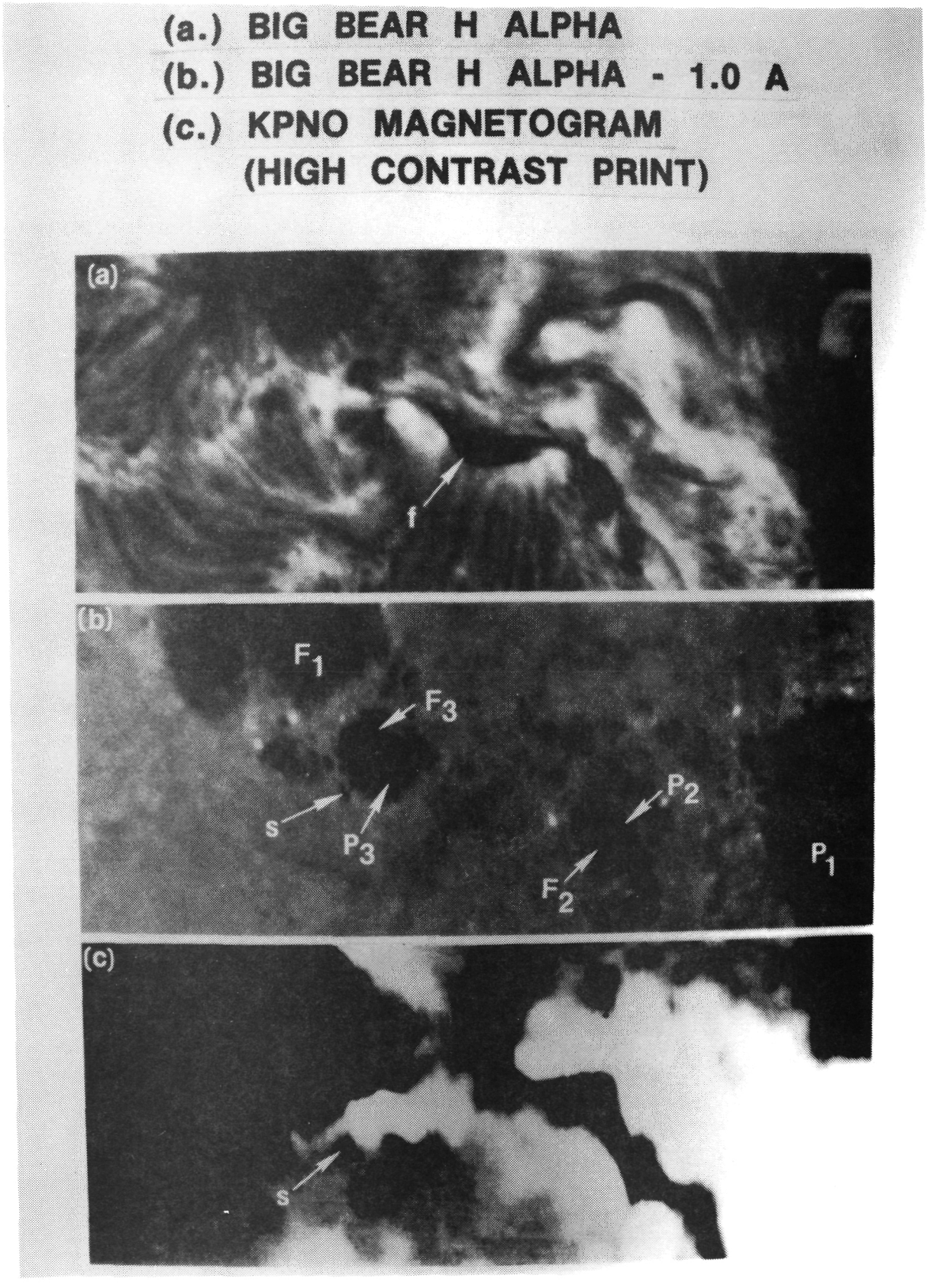

Figure 10. H-alpha spectroheliograms and KPNO magnetogram prior to the flare of April 10, 1980.

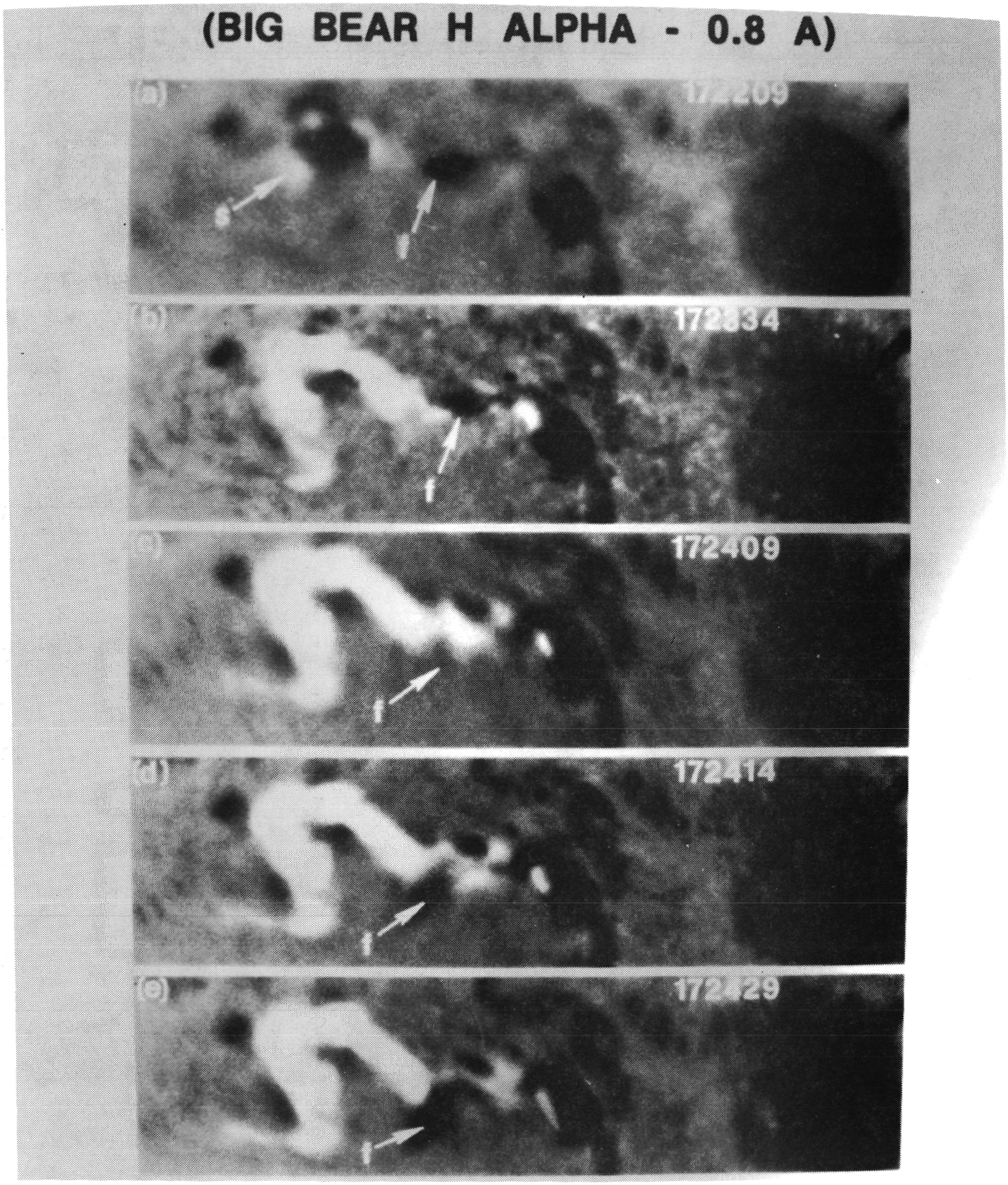

Figure 11. H-alpha spectroheliograms showing the onset and development of the flare of April 10, 1980.

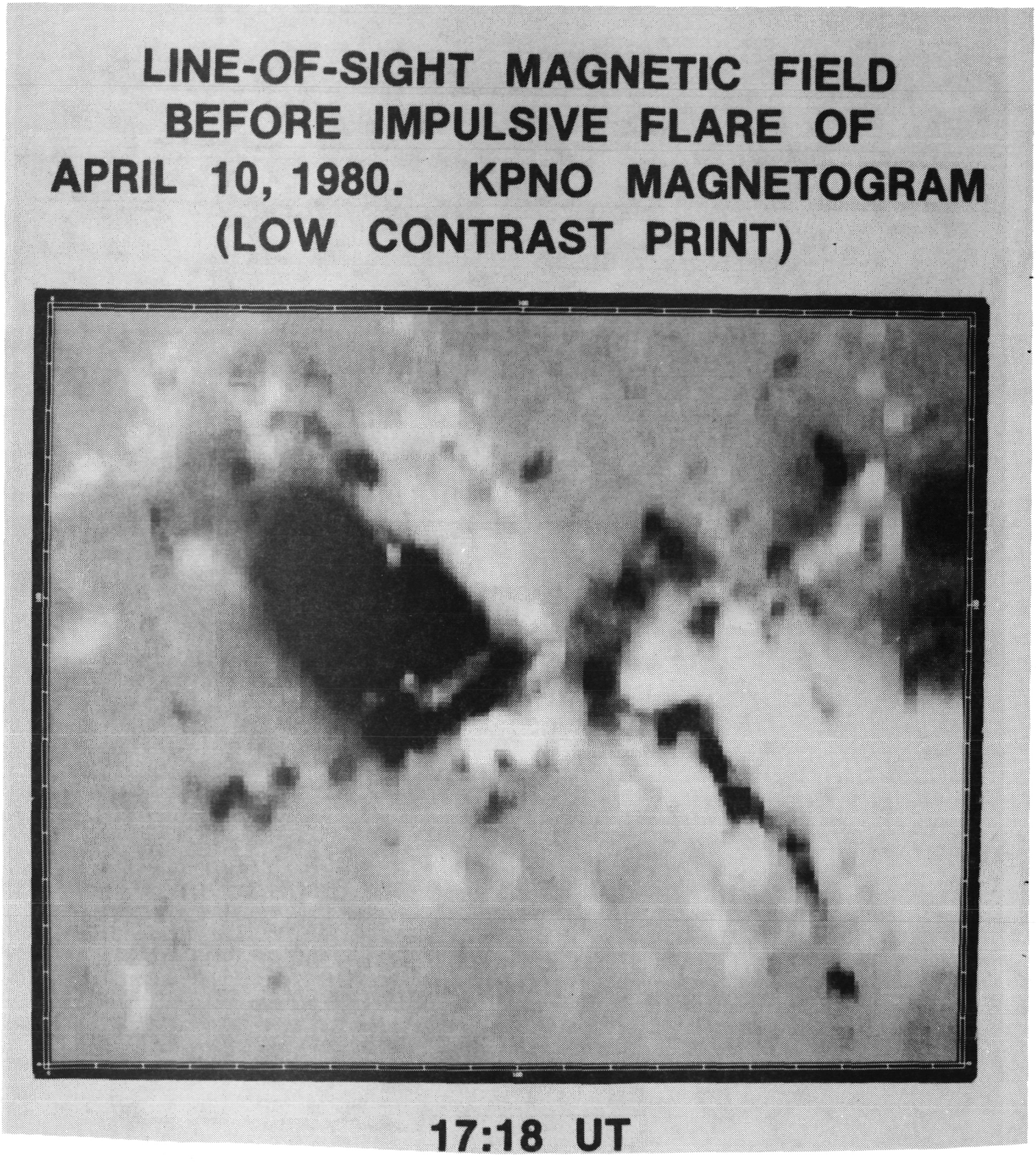

Figure 12. KPNO magnetogram of the line-of-sight magnetic field before the flare of April 10, 1980.

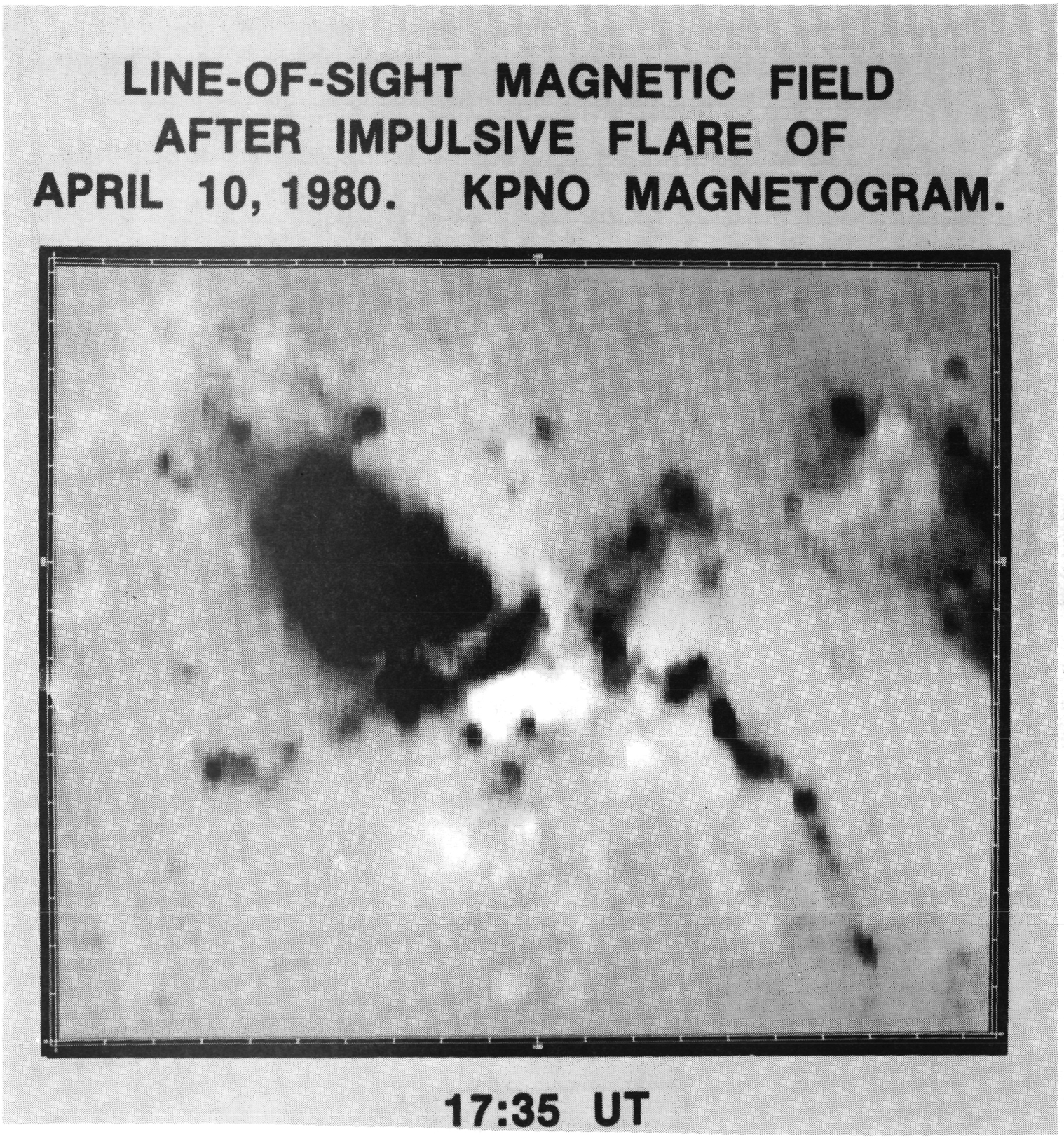

Figure 13. KPNO magnetogram of the line-of-sight magnetic field after the flare of April 10, 1980.

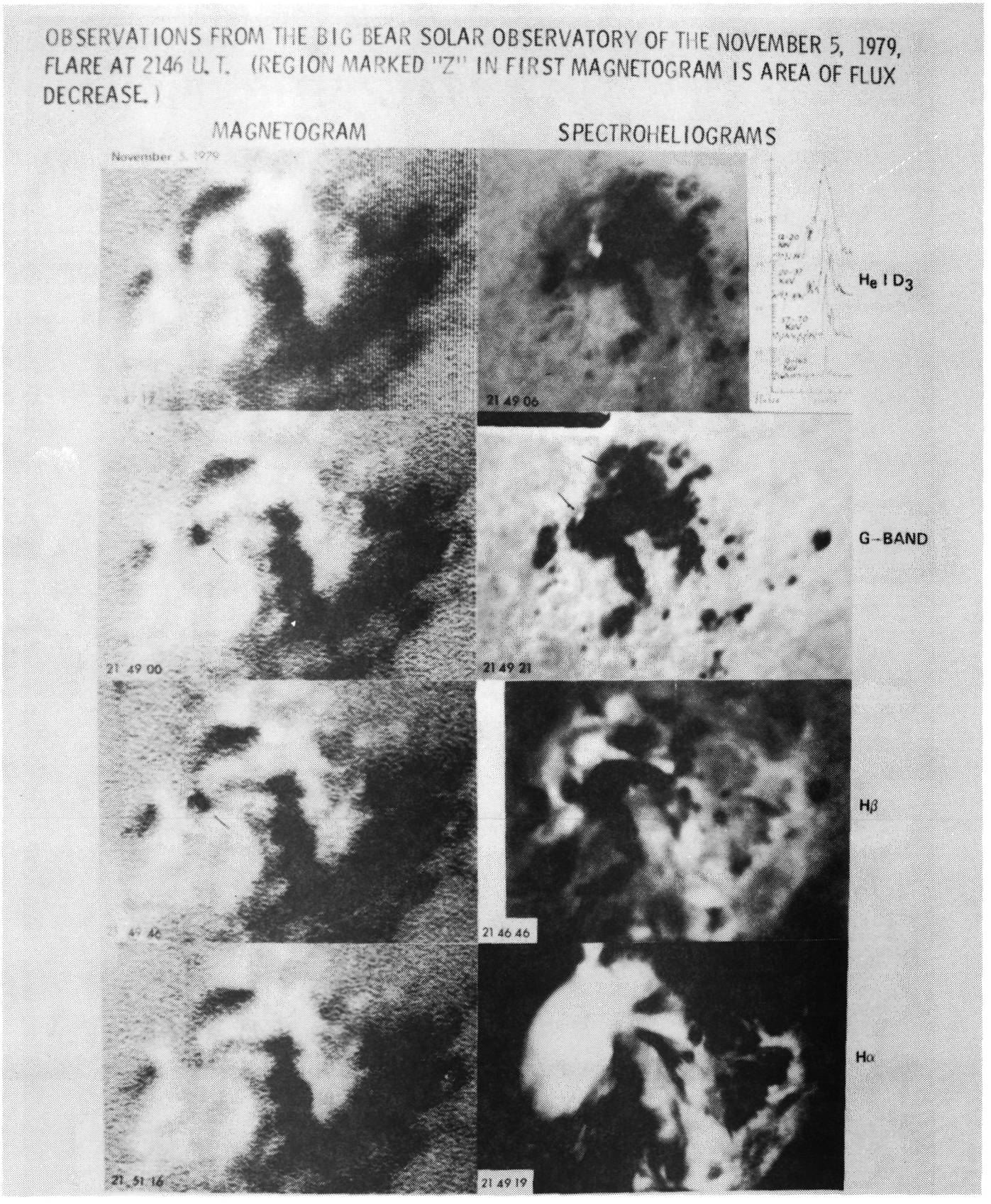

Figure 14. Line-of-sight magnetograms and spectroheliograms from the Big Bear Solar Observatory during the interval of the flare on November 5, 1979, at 2146 UT showing area of flux decrease.

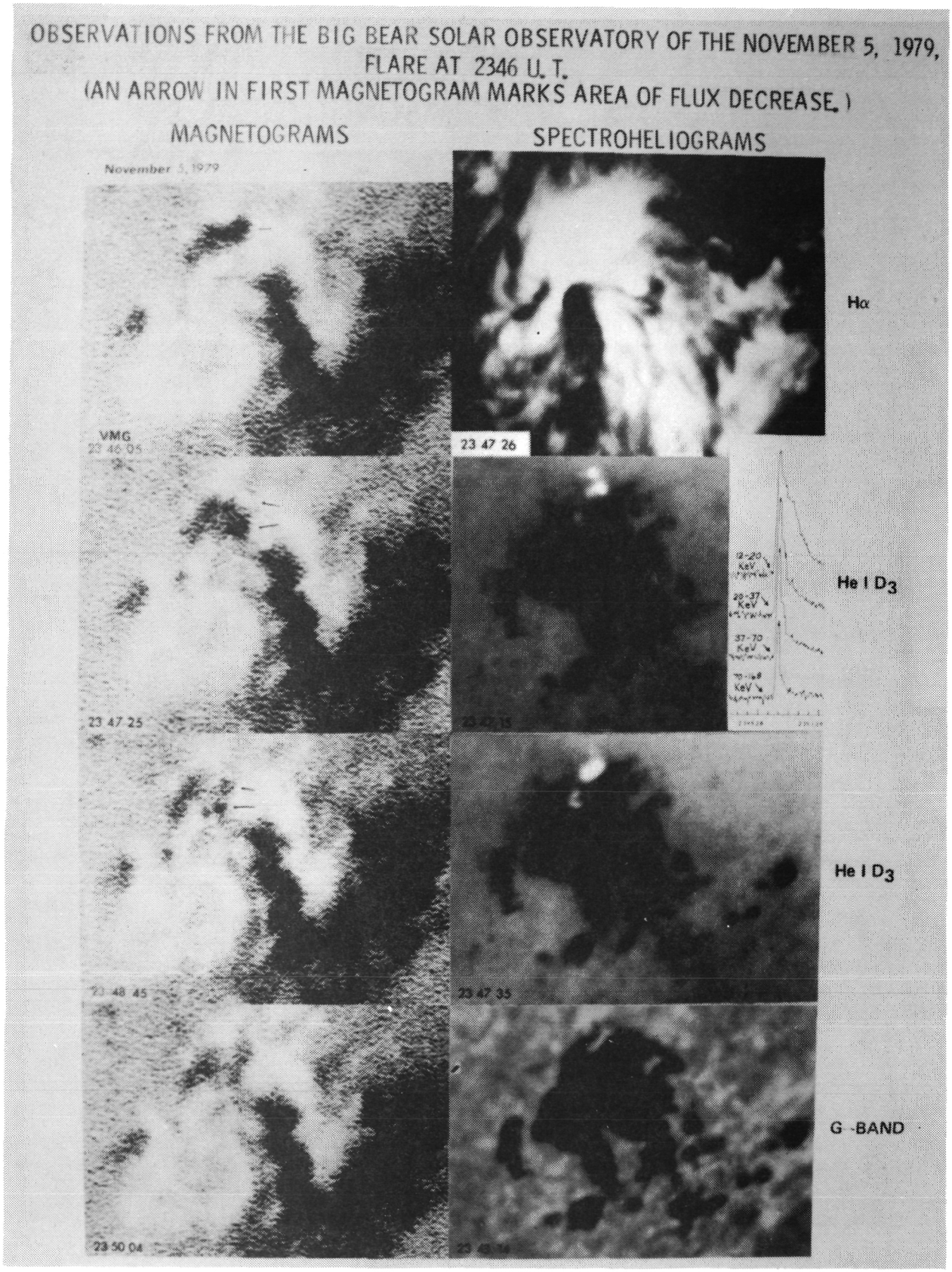

Figure 15. Line-of-sight magnetograms and spectroheliograms from BBSO during the interval of the second flare of November 5, 1979, at 2346 UT showing areas of flux decrease.

MAGNETIC TRANSIENT OBSERVATIONS WITH THE BIG BEAR SOLAR OBSERVATORY VIDEOMAGNETOGRAPH

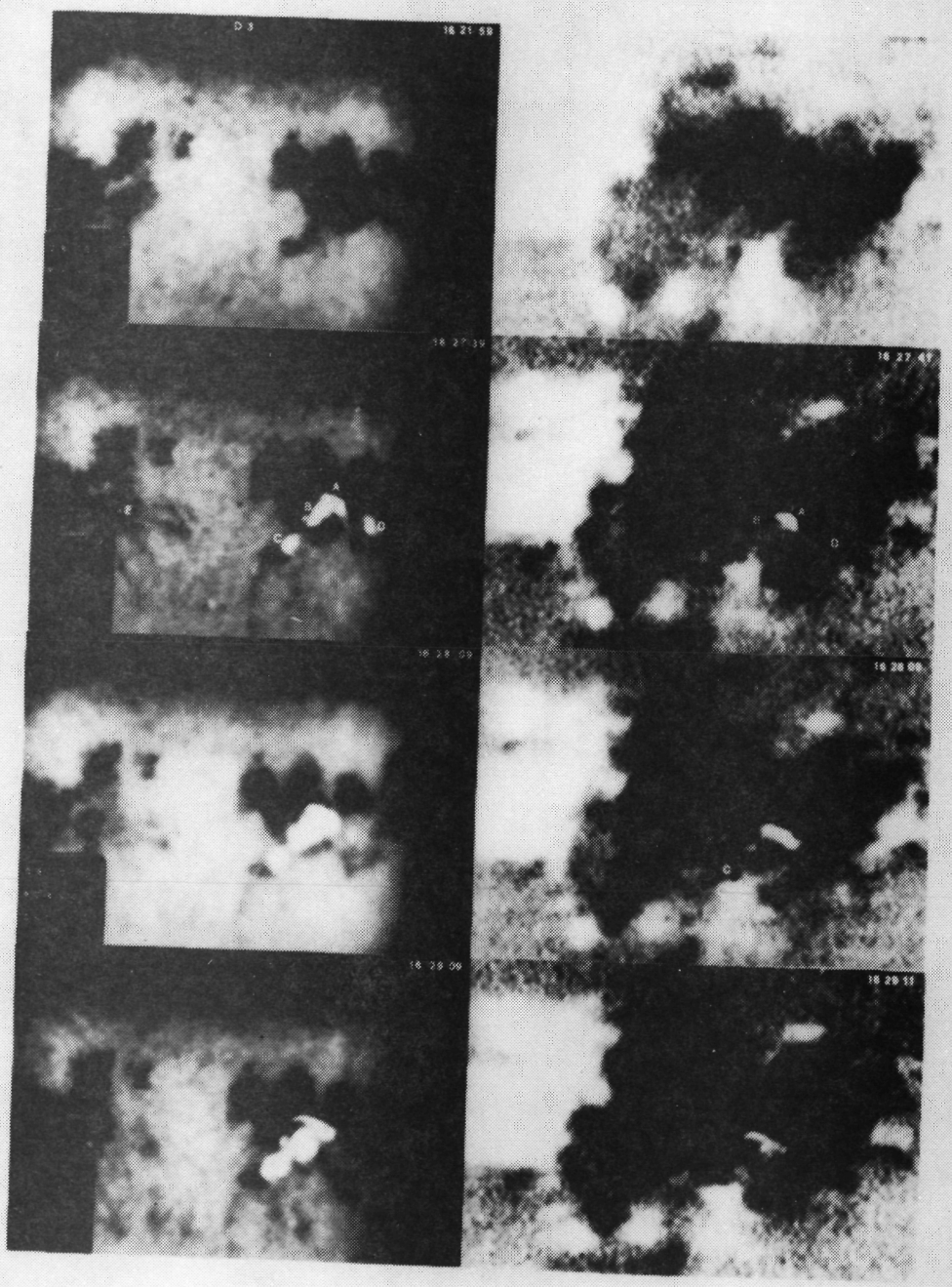

a. H_E D_3

b. Line-of-Sight Magnetic Field

Figure 16. Observations of a magnetic transient from BBSO: magnetograms and He D_3 spectroheliograms.

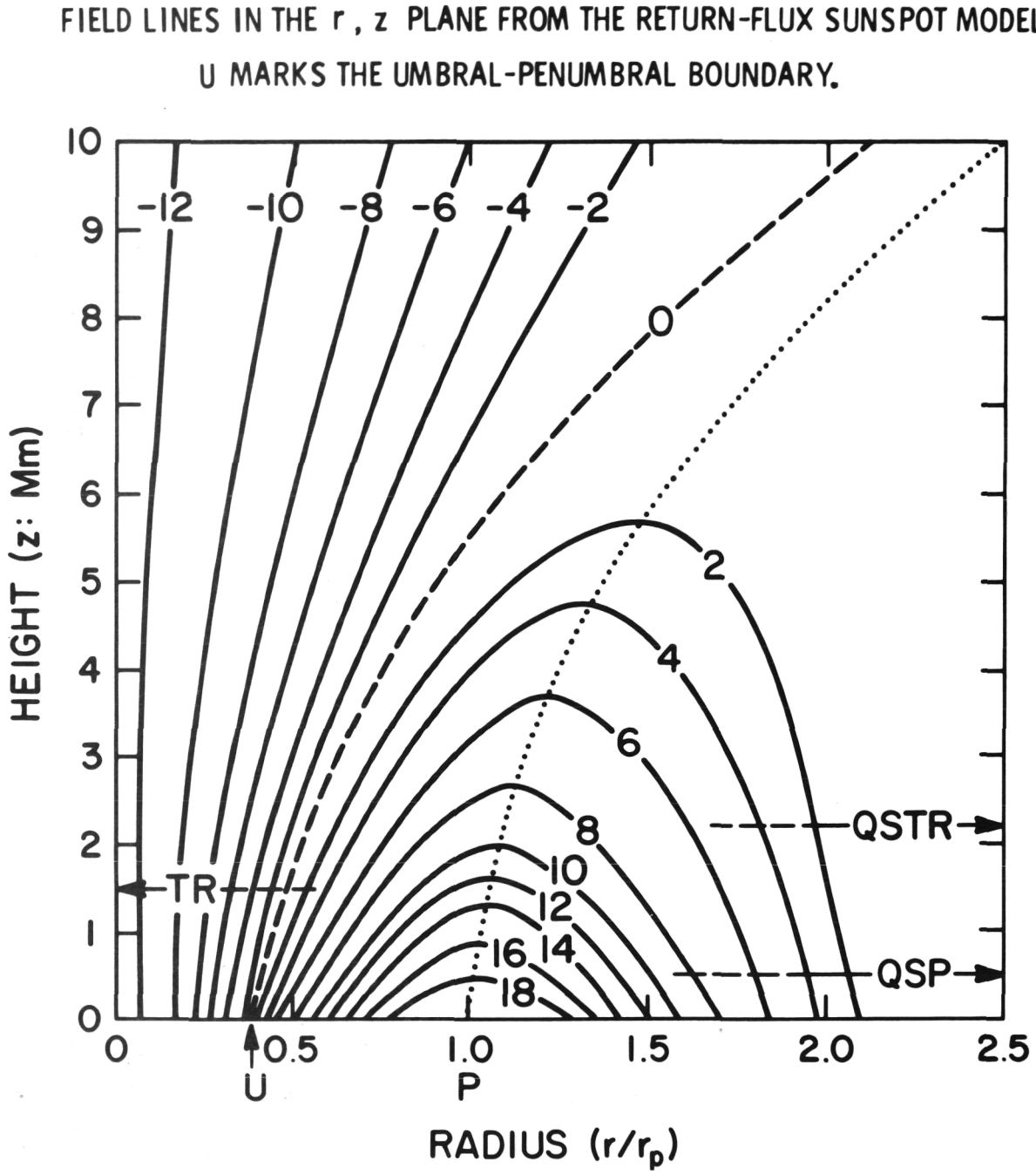

Figure 17. Distribution of field lines in the r-z plane from the "return flux" sunspot model showing regions of open and closed field lines.

MAGNETIC FIELD STRUCTURE DERIVED FROM THE RETURN-FLUX SUNSPOT MODEL

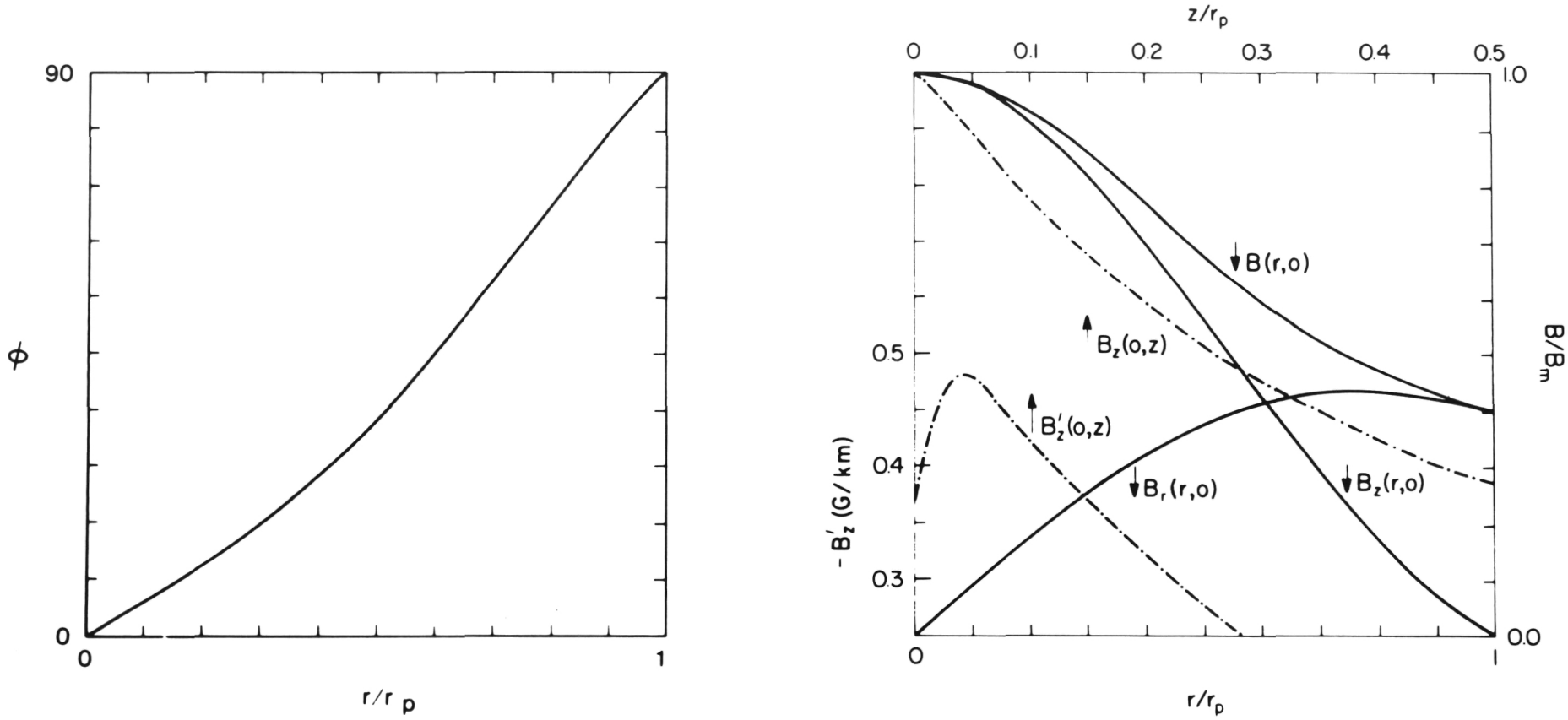

a. DERIVED RADIAL DISTRIBUTION OF THE FIELD INCLINATION ANGLE ϕ

b. VARIATION OF B_r, B_Z, B ALONG SUNSPOT RADIUS AT Z O; VARIATION OF B_Z WITH Z AT r O.

Figure 18. Variations with r and z of components of the magnetic field derived from the "return flux" model.

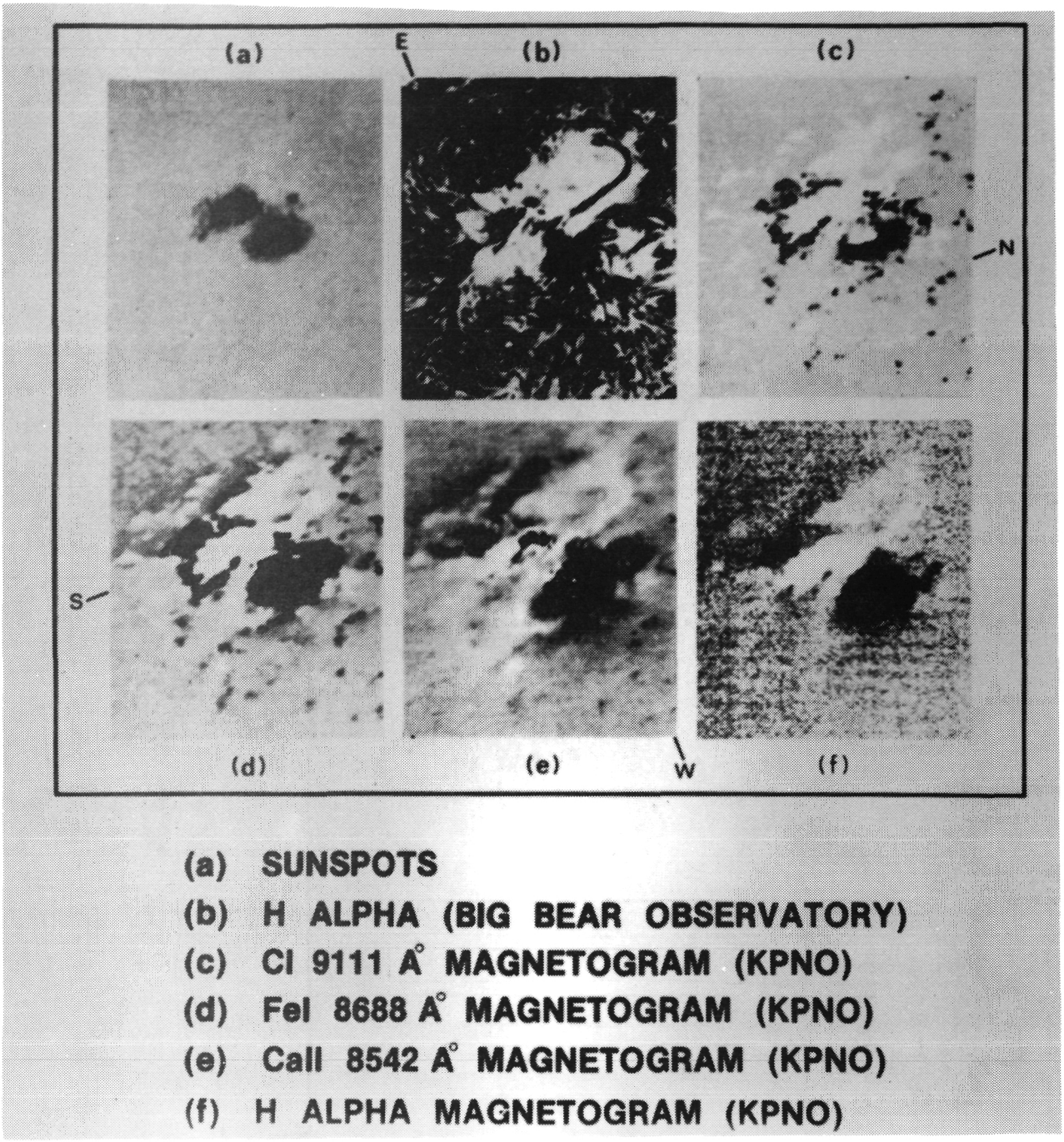

Figure 19. KPNO magnetograms in different spectral lines and BBSO H-alpha spectroheliograms showing the magnetic fields at different heights above a sunspot.

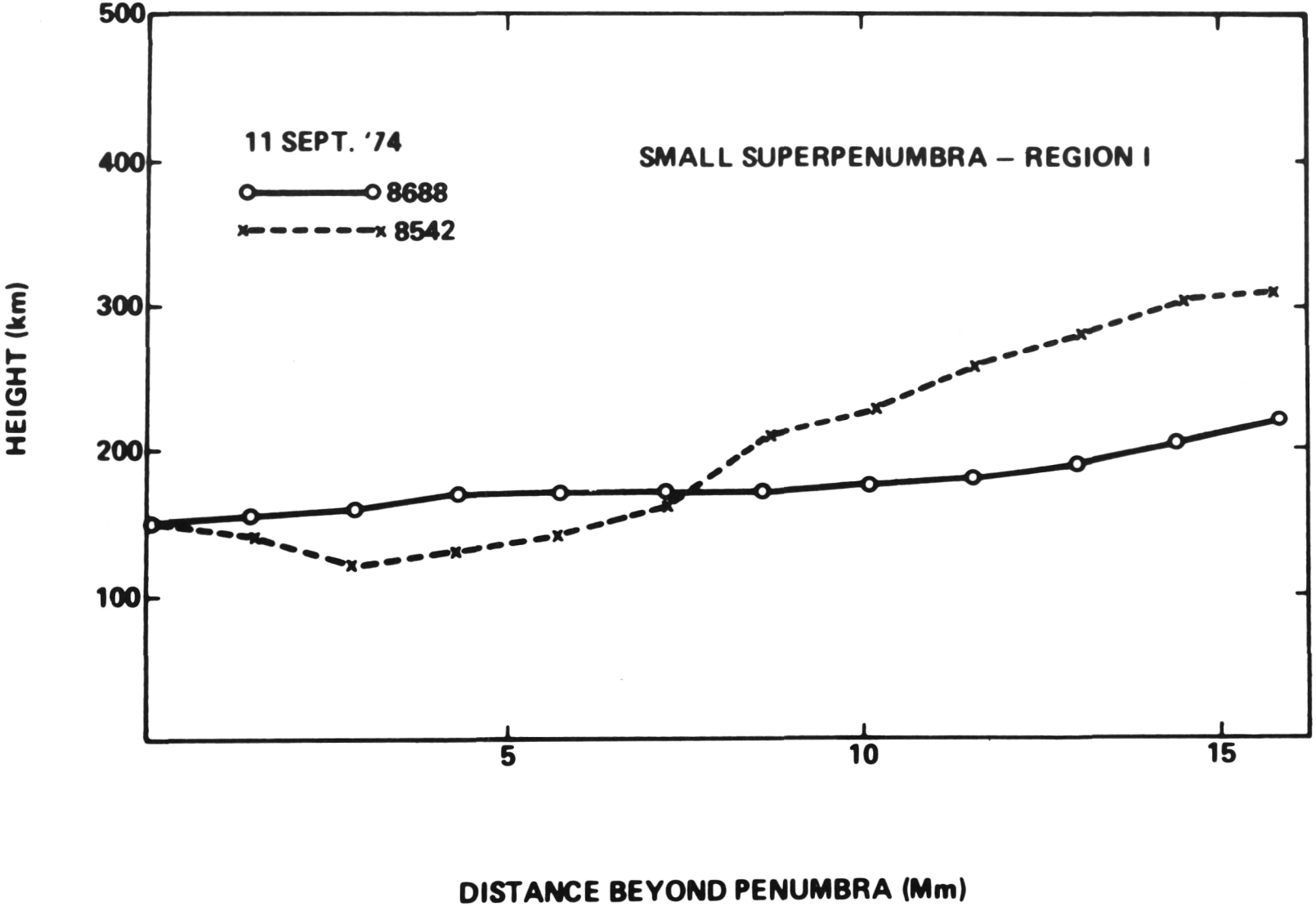

Figure 20. Variation with distance of the height of the magnetic canopy over a small superpenumbral region.

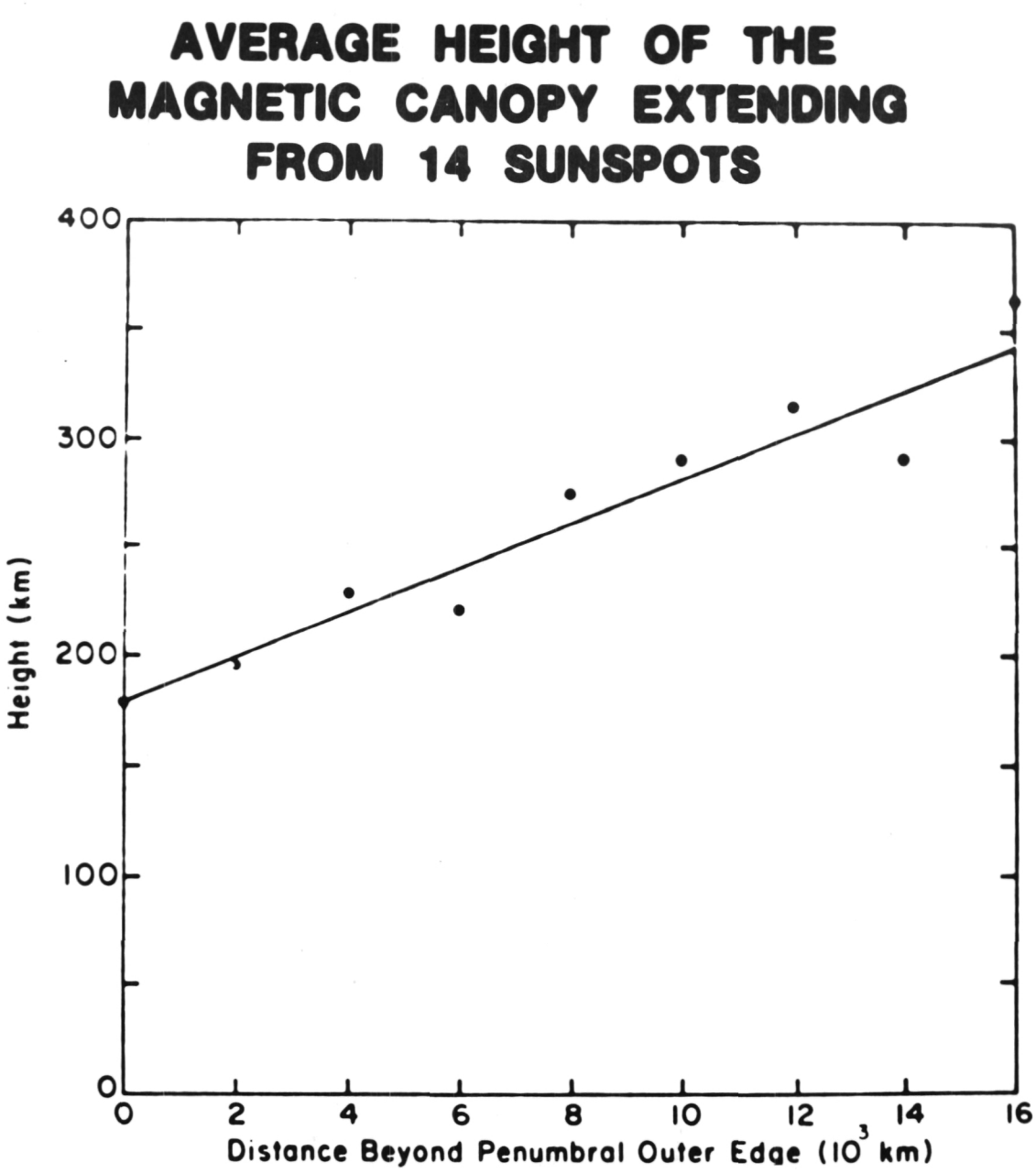

Figure 21. Average variation with distance of the height of magnetic canopies extending from sunspots.

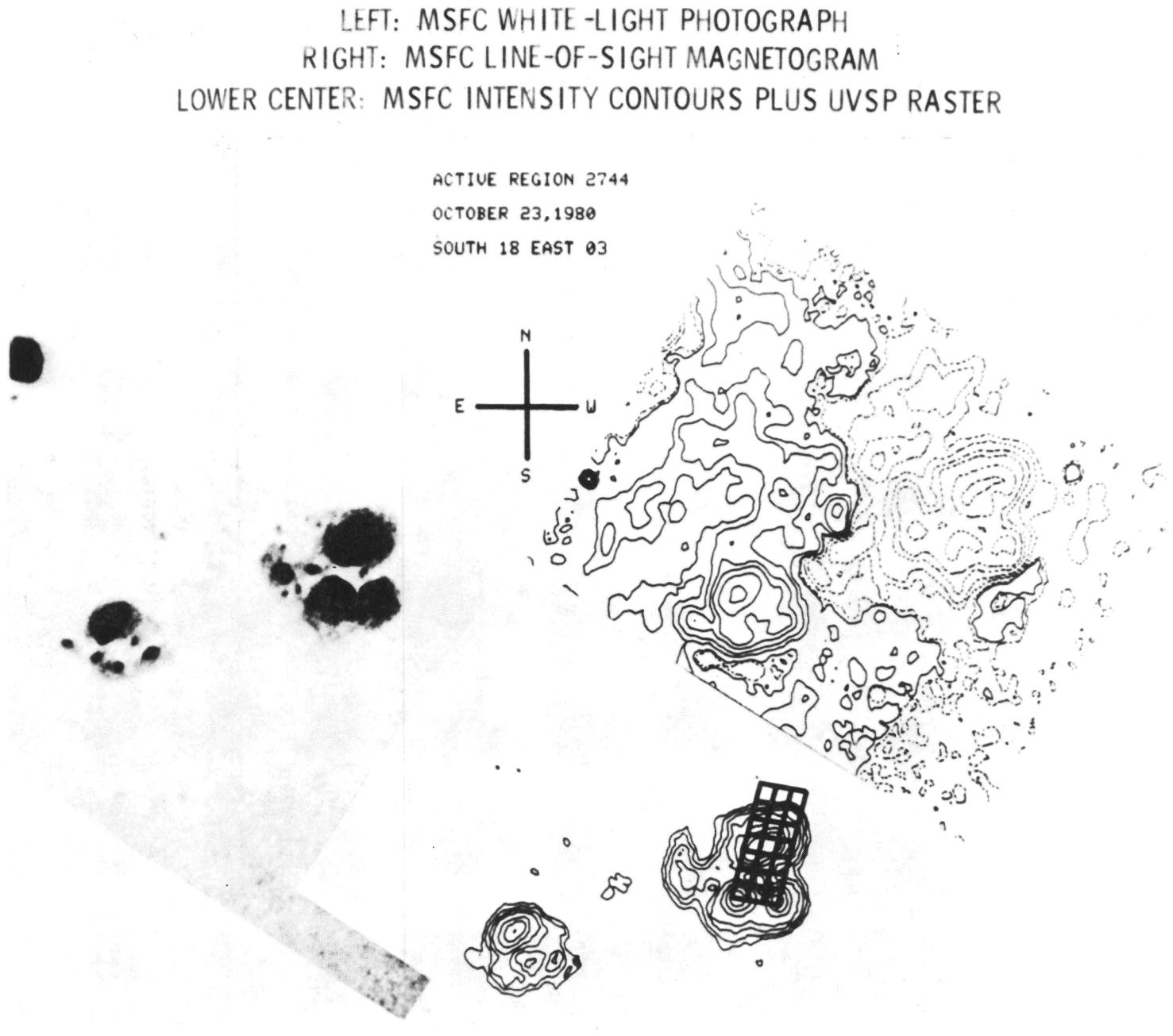

Figure 22. Observed sunspot and line-of-sight magnetogram of active region 2744 on October 23, 1980; position of the UVSP raster is shown superimposed on intensity contours of the sunspot.

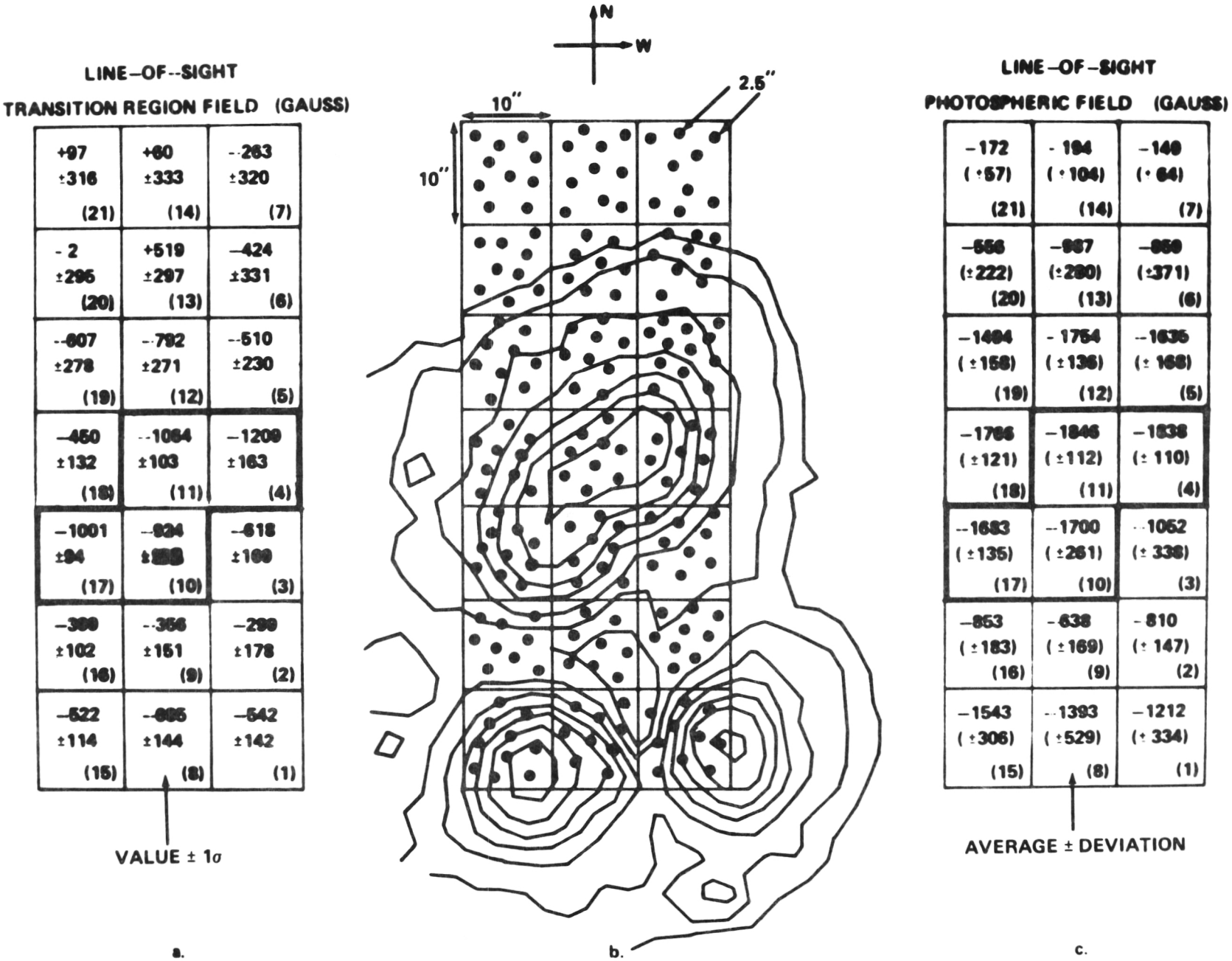

Figure 23. Line-of-sight magnetic fields in the photosphere and transition region for active region 2744 on October 23, 1980.

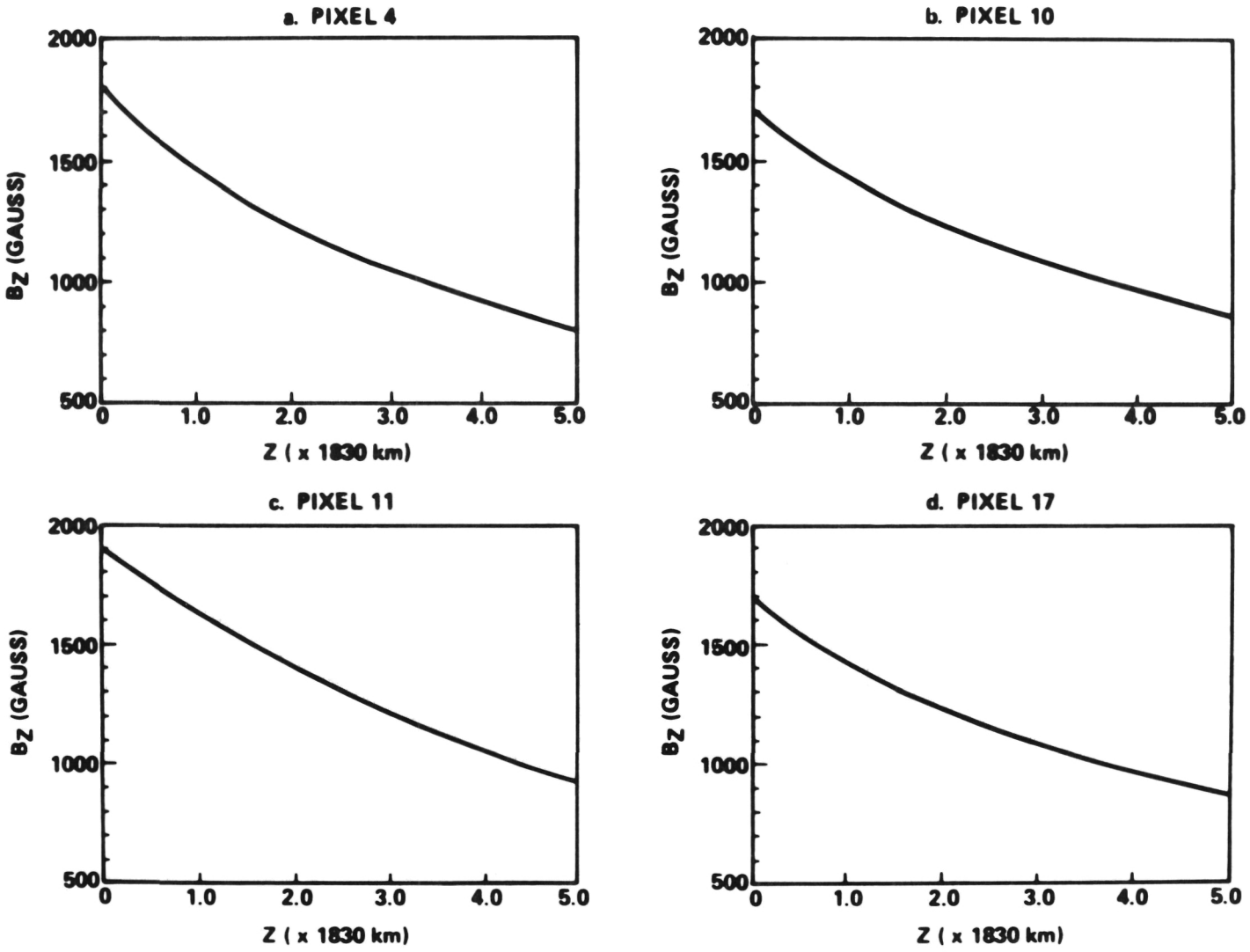

Figure 24. Plots of the variation with height of the z-component of a potential field for the sunspot in active region 2744 at four locations.

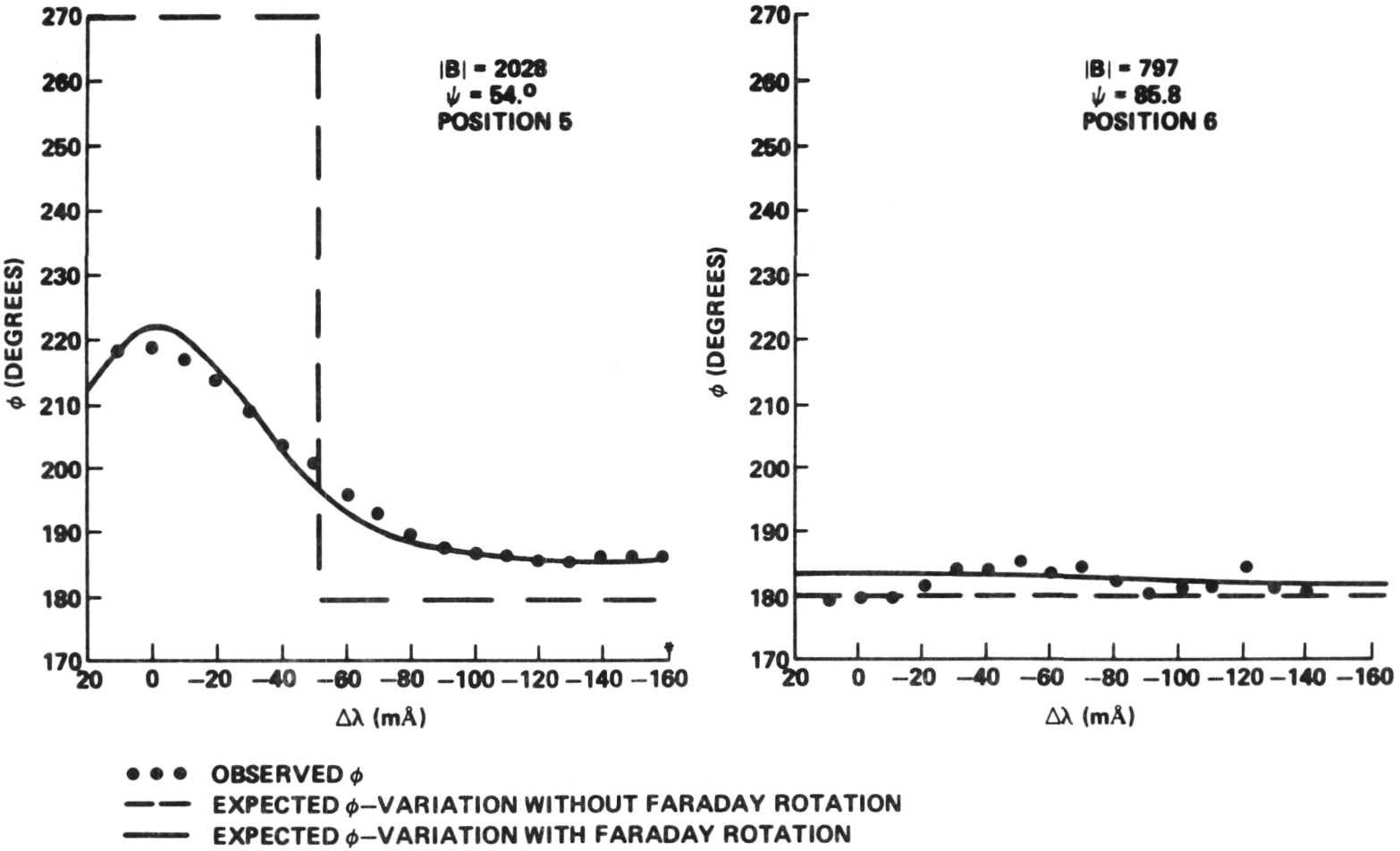

Figure 25. Observations of Faraday rotation of the azimuth of the transverse magnetic field in a sunspot.

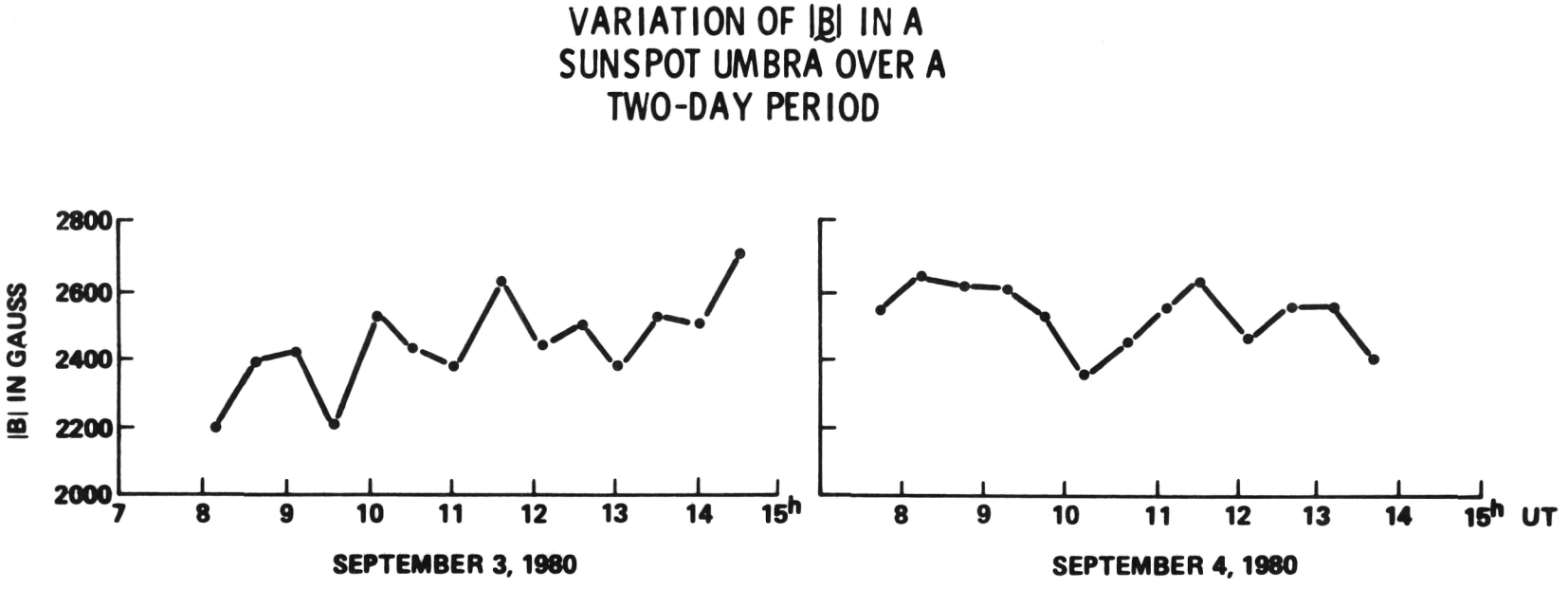

Figure 26. Potsdam Tower Telescope observations of umbral field magnitudes.

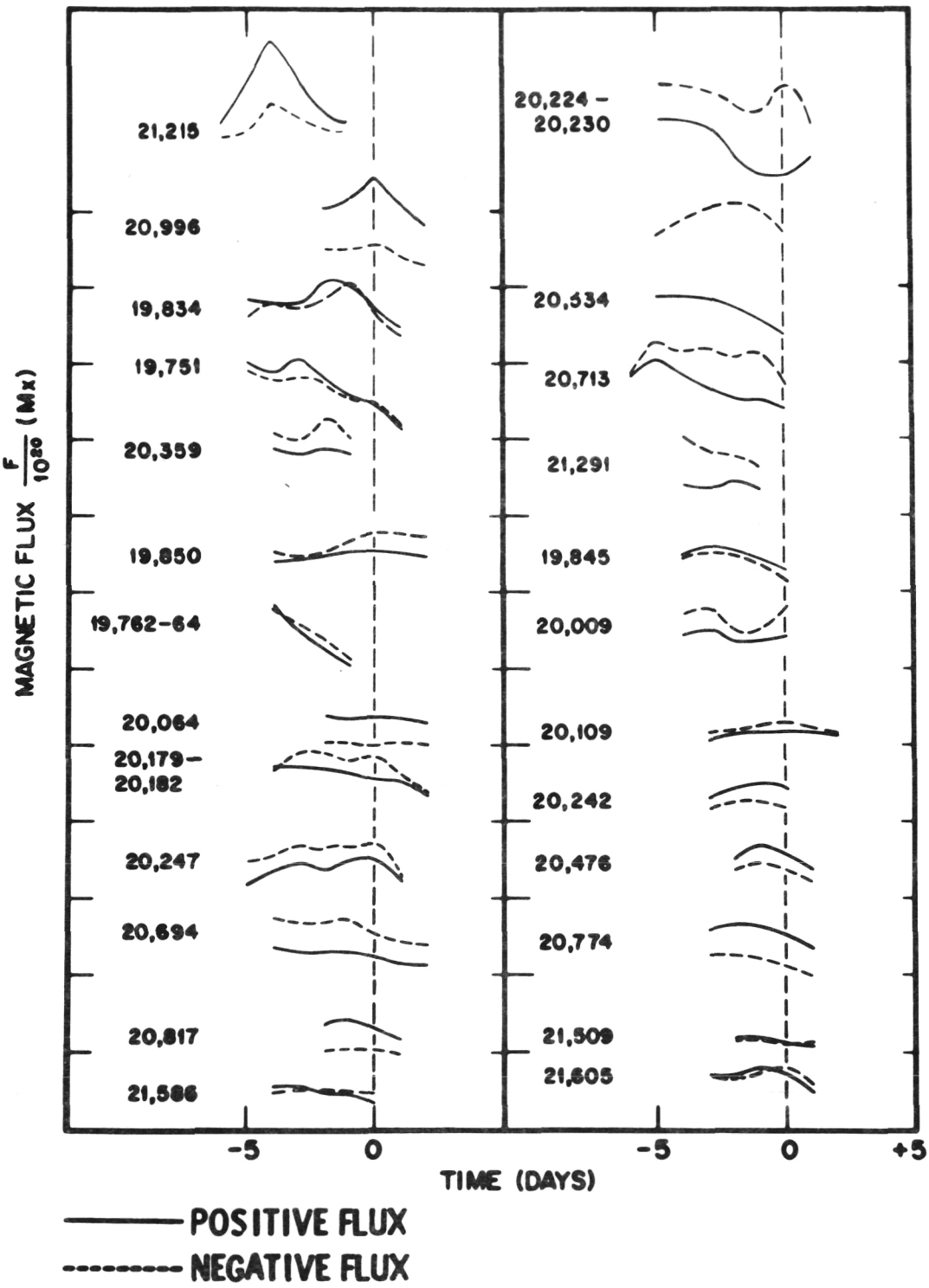

Figure 27. Mount Wilson observations of positive and negative flux as a function of time during the interval of time in which 25 sunspots disappeared.

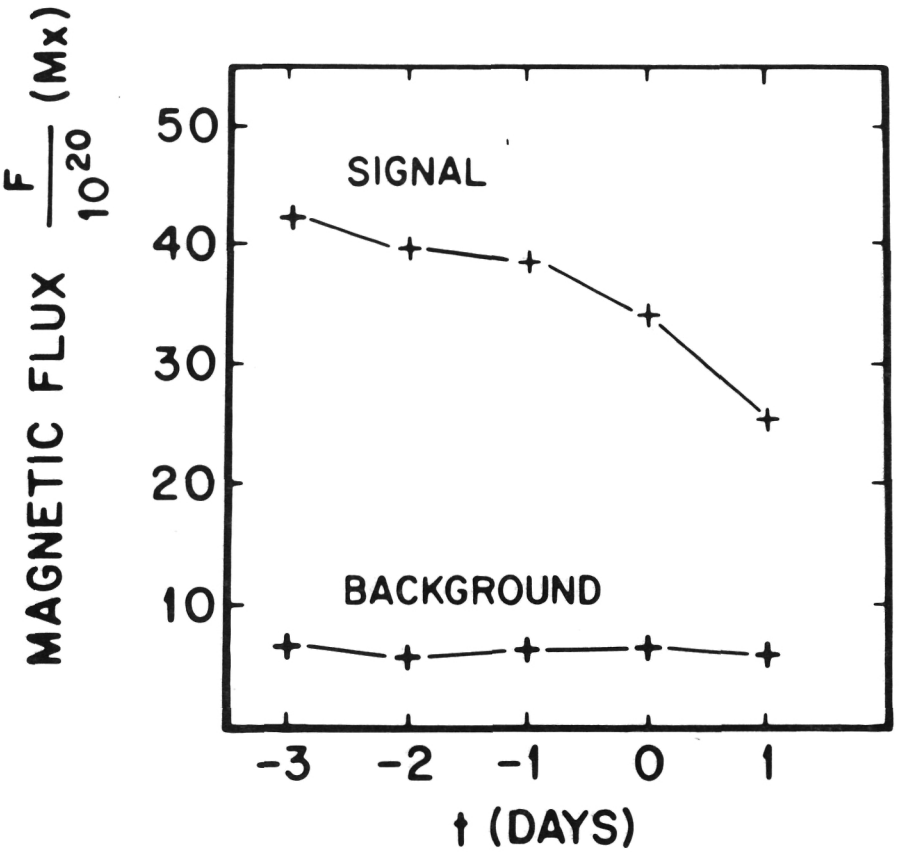

SIGNAL ≡ TOTAL FLUX MINUS WEAK-FIELD FLUX (< 10G)

BACKGROUND ≡ WEAK-FIELD FLUX

Figure 28. Plot of average flux versus time during the interval of time in which the 25 sunspots disappeared.

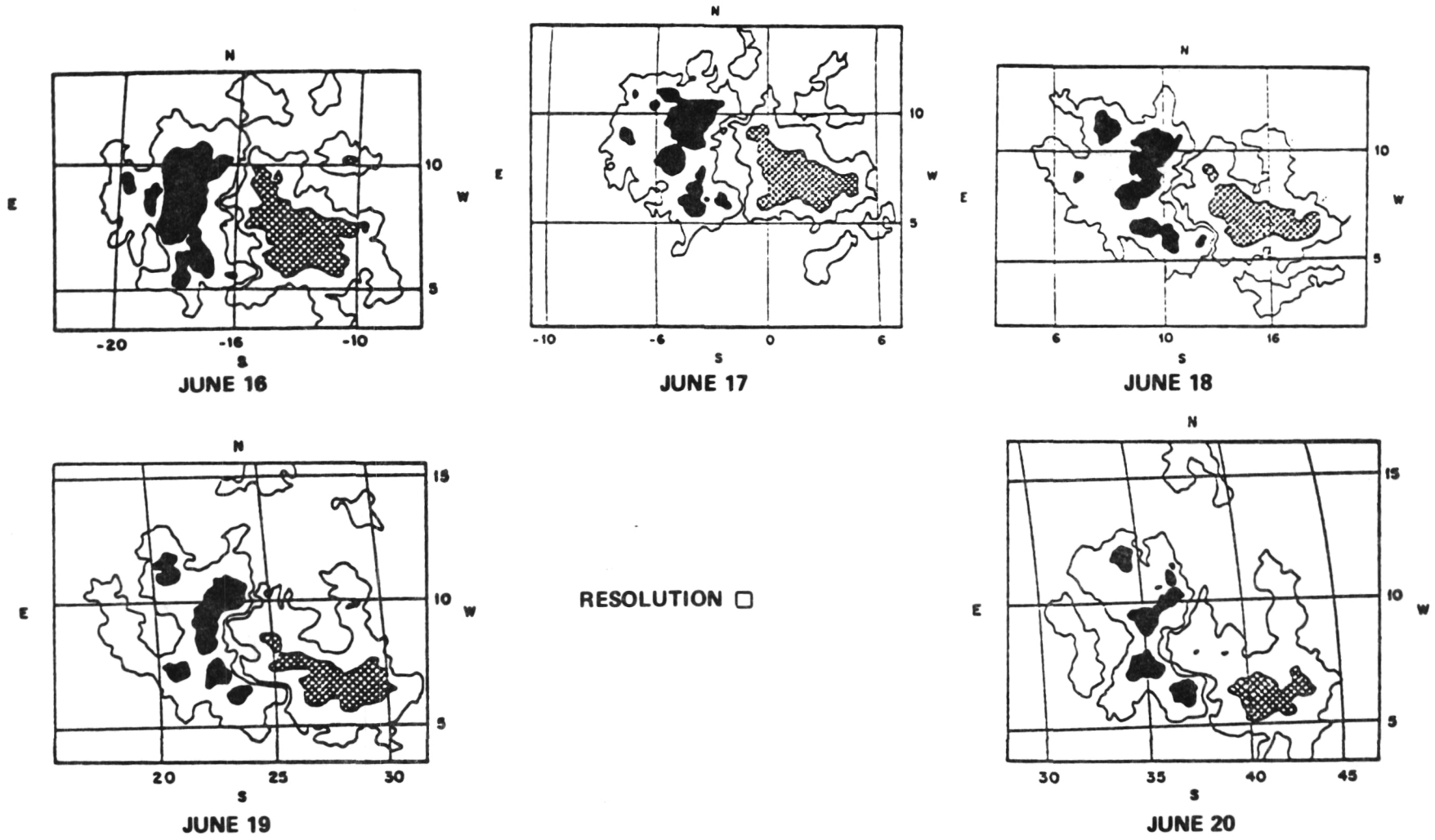

Figure 29. Mount Wilson magnetograms of active region 17694 for the period June 16-20, 1981.

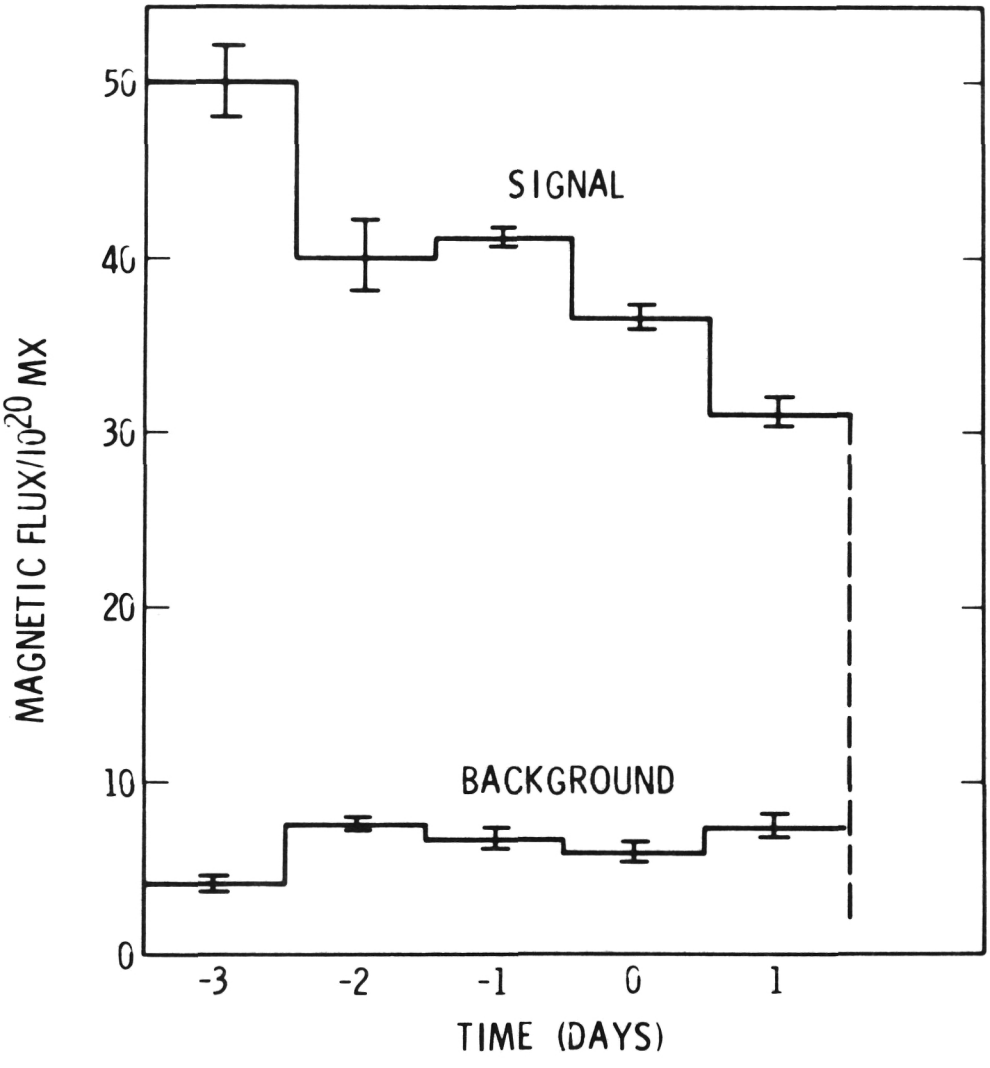

Figure 30. Plot of negative flux versus time during the interval of time in which the sunspot of active region 17694 disappeared (June 16-20, 1981).

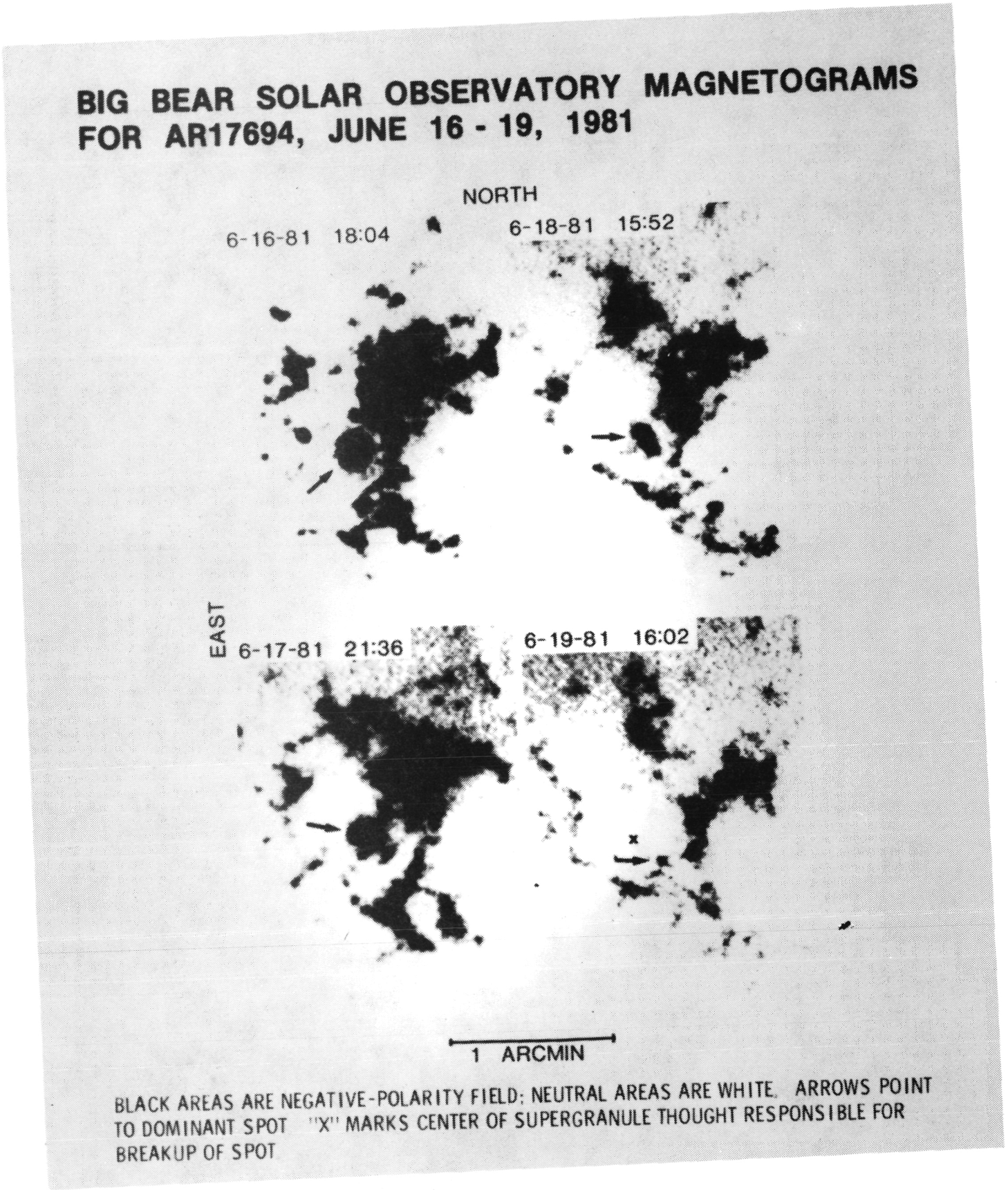

Figure 31. BBSO magnetograms for active region 17694 during the time interval June 16-19, 1981.

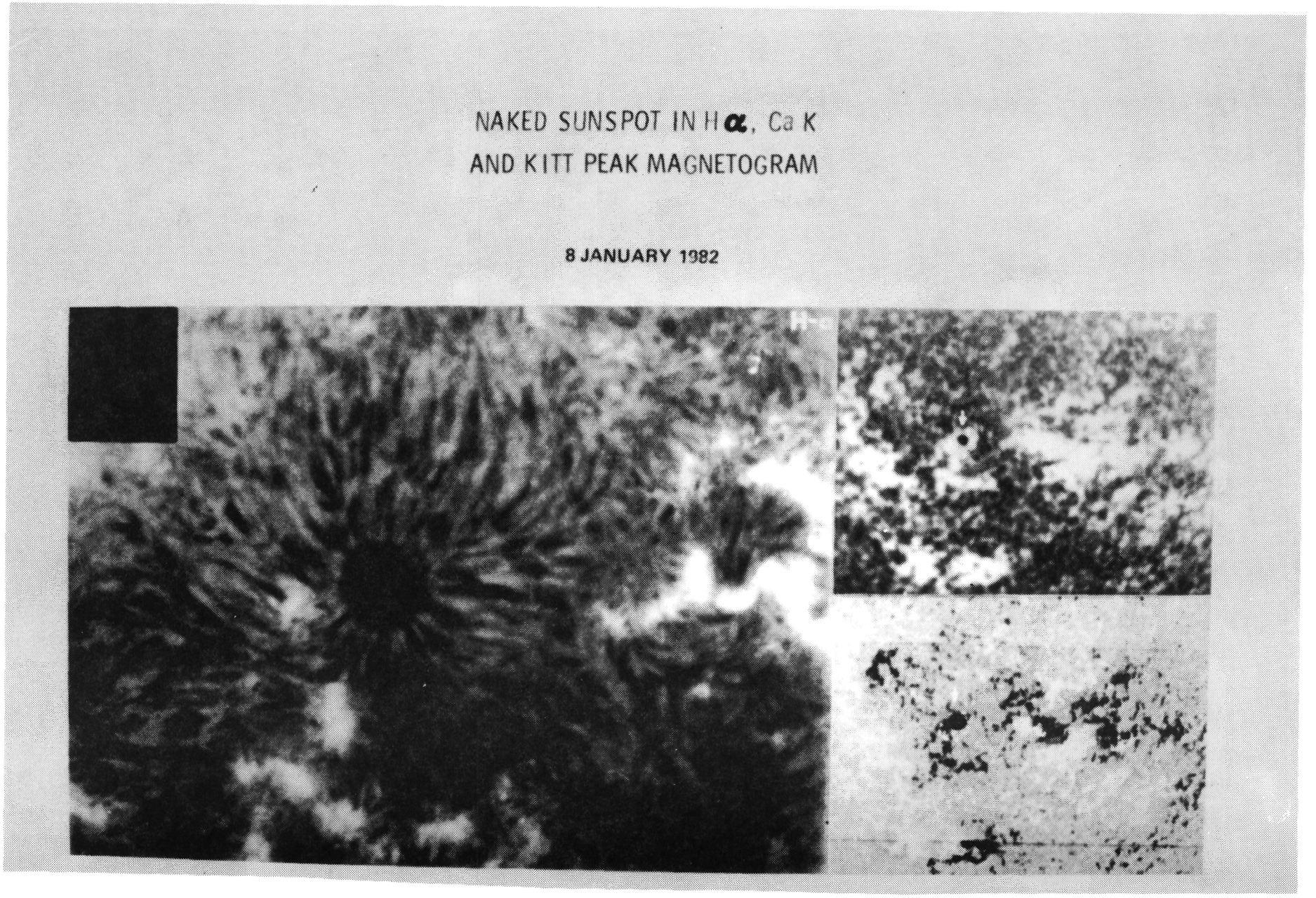

Figure 32. Example of a "naked" sunspot in H-alpha and Ca K spectroheliograms, together with a KPNO magnetogram.

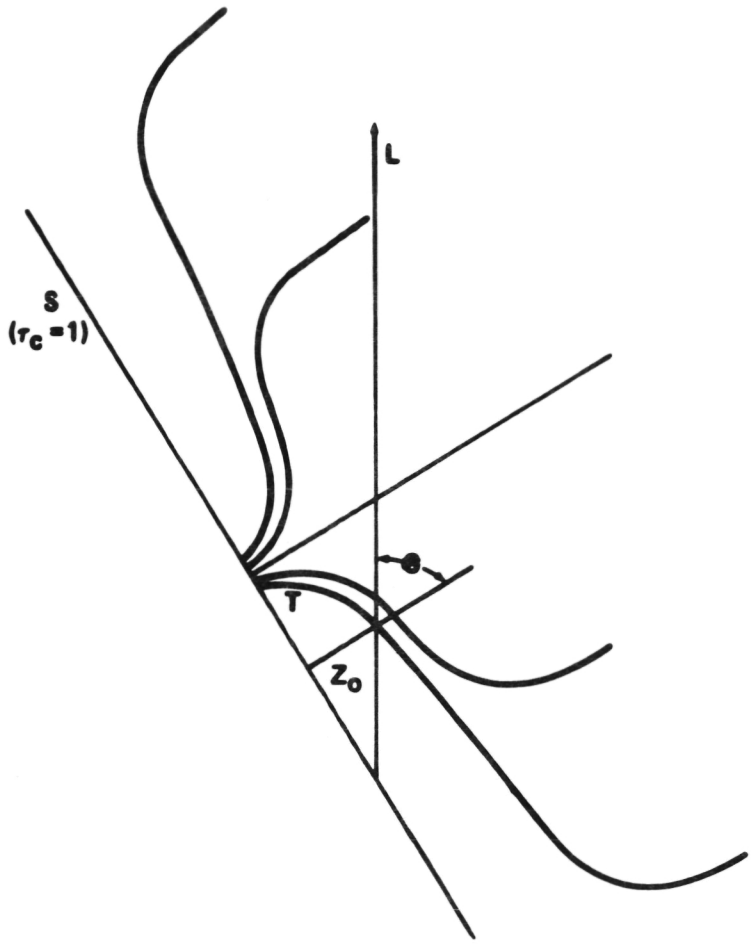

Figure 33. Illustration of the field configuration of a magnetic "canopy" extending over the supergranular network.

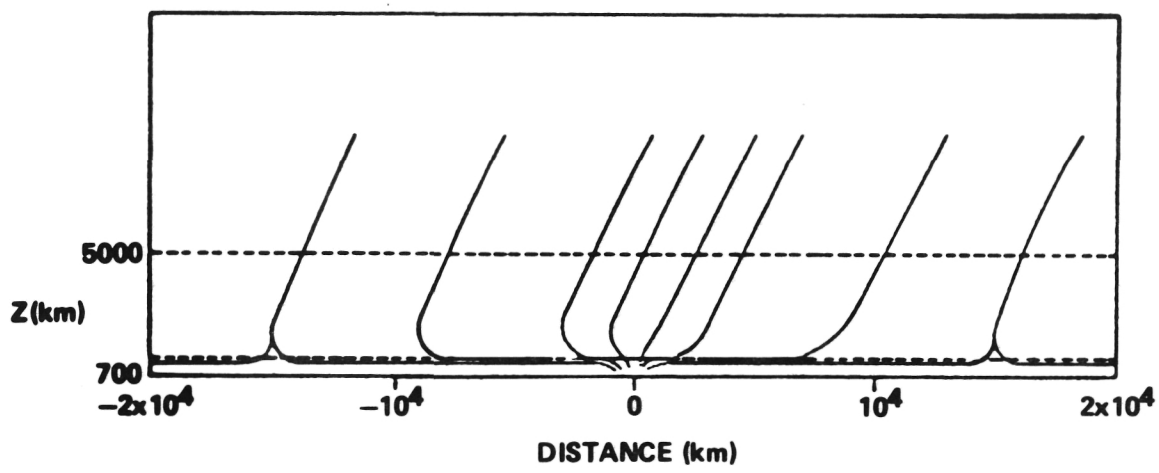

Figure 34. Large-scale illustration of the magnetic field configuration of network cells.

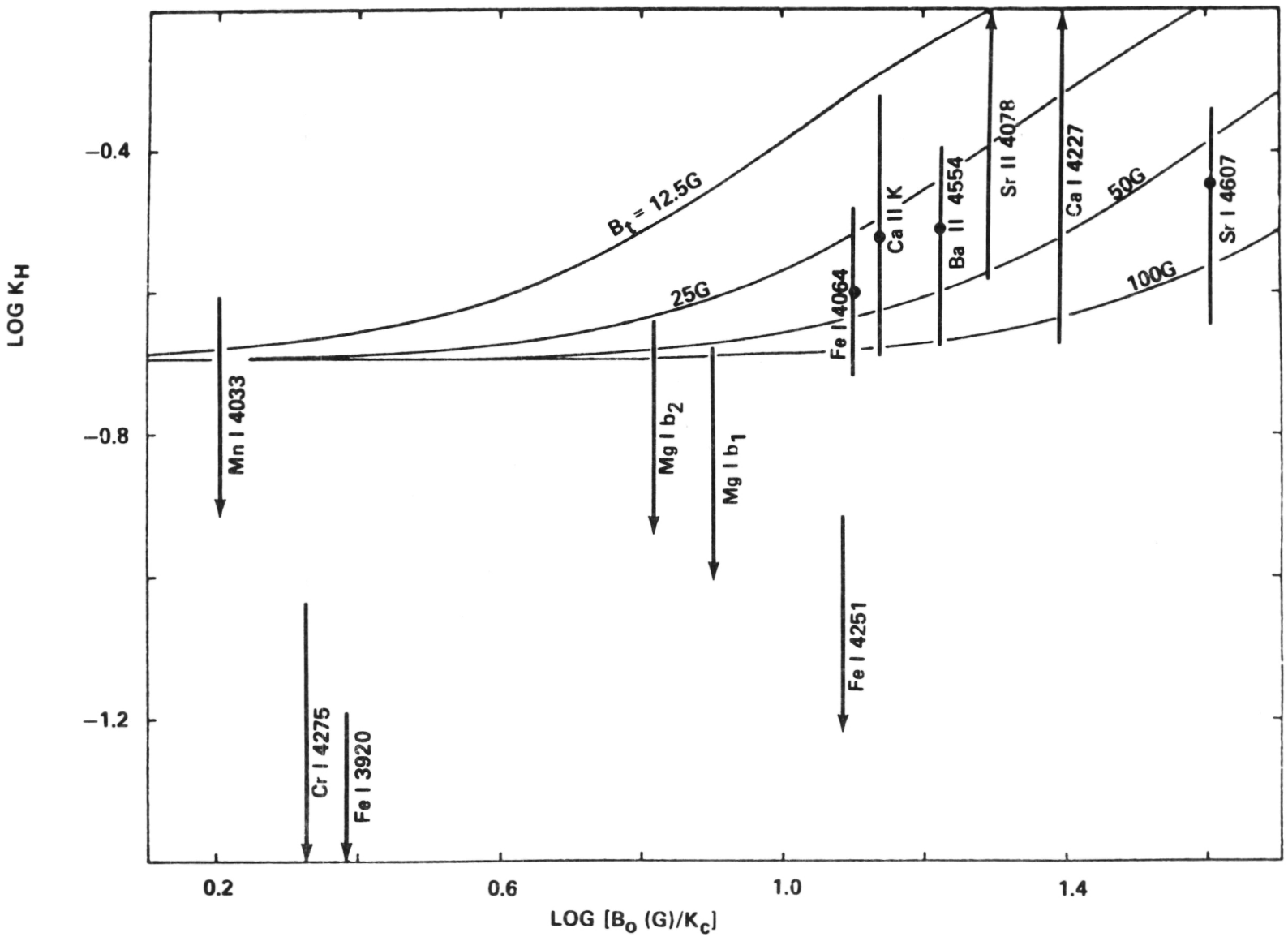

Figure 35. Plot of derived values of the Hanle depolarization, k_H versus calculated values of the collisional depolarization k_c, with the turbulent magnetic field B_t as parameter. Also shown are results of observed depolarizations.

a. PROMINENCES OBSERVED EDGE–ON
b. ASSUMPTION OF A KUPERUS–RAADU MODEL
c. ASSUMPTION OF A KIPPENHAHN–SCHLUTER MODEL

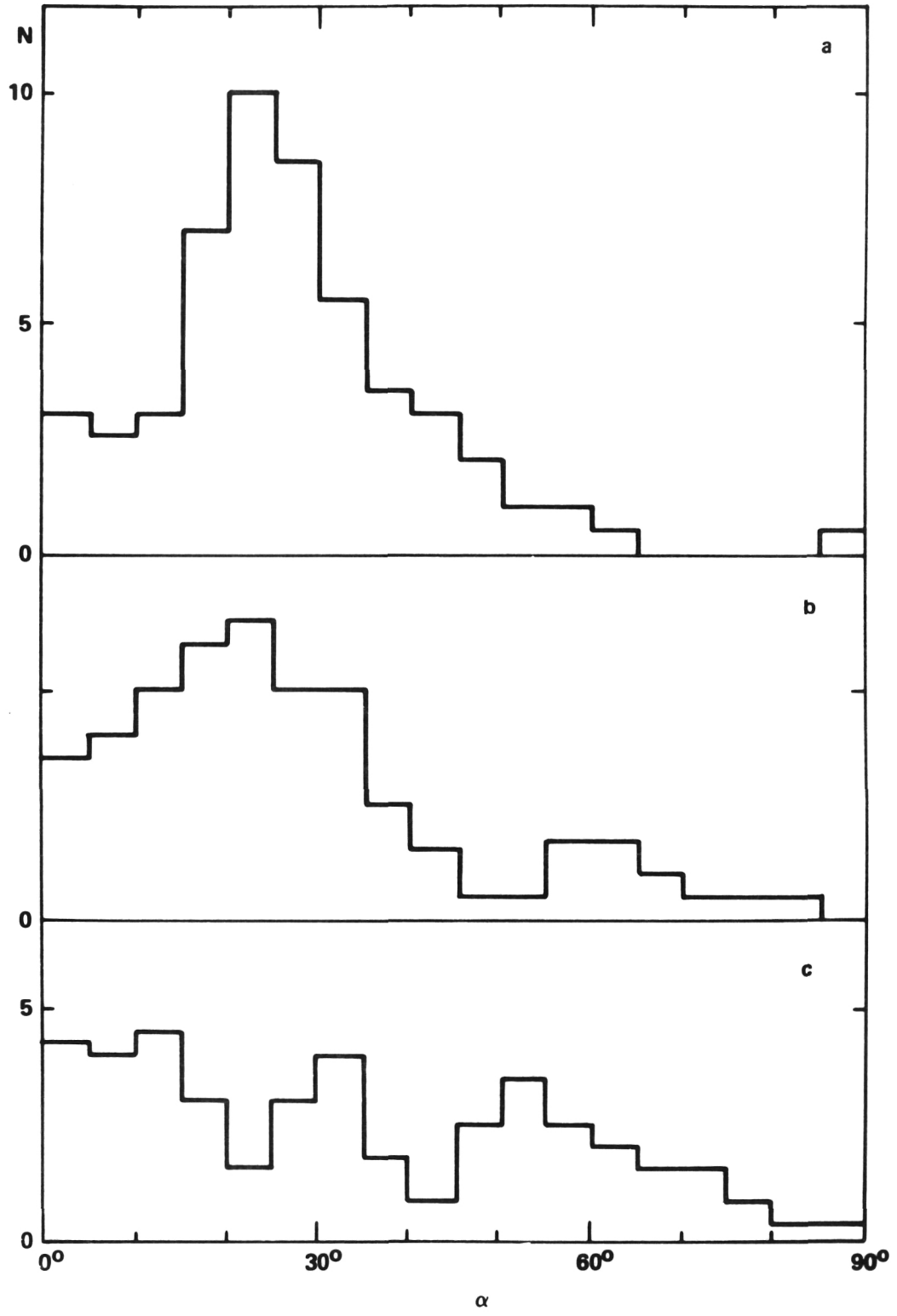

Figure 36. Orientation of the transverse magnetic field in solar prominences.

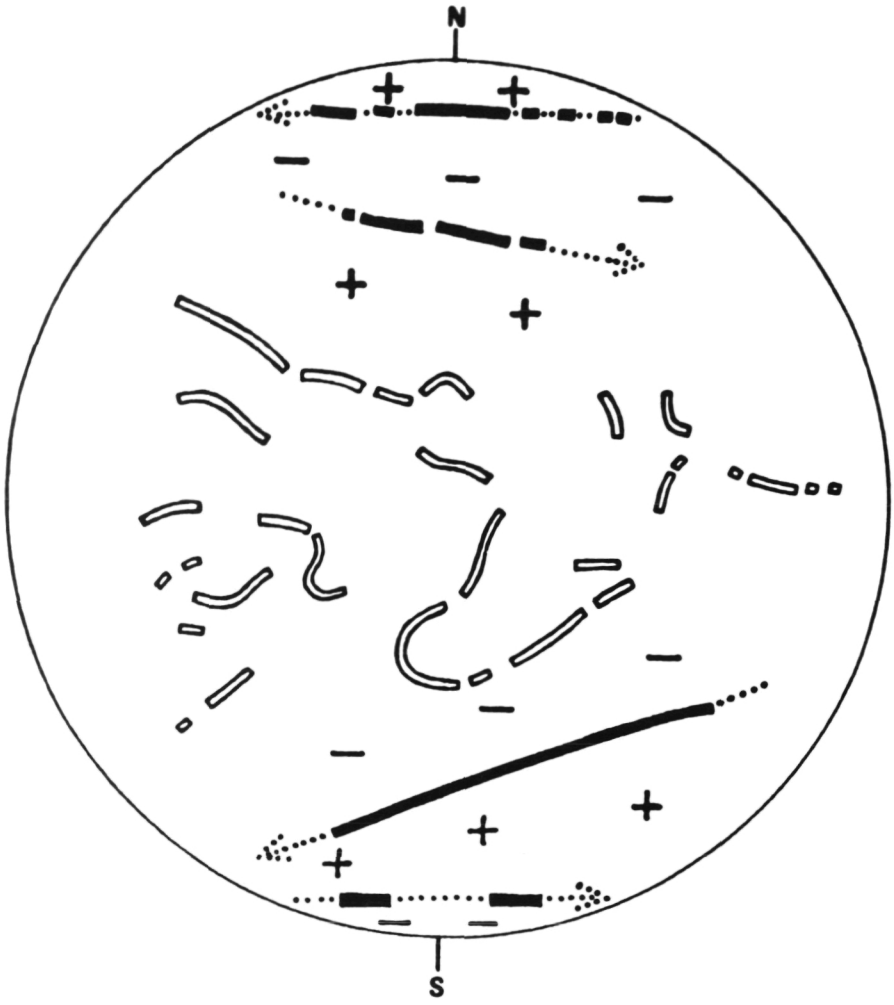

Figure 37. Observation of the transitional period in the cyclic change of solar prominence magnetic fields: directions of prominence and photospheric magnetic fields on July 15, 1980.

APPROVAL

STUDIES OF SOLAR MAGNETIC FIELDS DURING THE SOLAR MAXIMUM YEAR

By M. J. Hagyard

The information in this report has been reviewed for technical content. Review of any information concerning Department of Defense or nuclear energy activities or programs has been made by the MSFC Security Classification Officer. This report, in its entirety, has been determined to be unclassified.

A. J. DESSLER
Director, Space Science Laboratory

☆U.S. GOVERNMENT PRINTING OFFICE 1984—544-048/10038